

Reduced Wave Green's Functions and Their Effect on the Dynamics of a Spike for the Gierer-Meinhardt Model

Theodore Kolokolnikov¹, Michael J. Ward²

Abstract

In the limit of small activator diffusivity ε , a formal asymptotic analysis is used to derive a differential equation for the motion of a one-spike solution to a simplified form of the Gierer-Meinhardt activator-inhibitor model in a two-dimensional domain. The analysis, which is valid for any finite value of the inhibitor diffusivity D with $D \gg \varepsilon^2$, is delicate in that two disparate scales ε and $-1/\ln \varepsilon$ must be treated. This spike motion is found to depend on the regular part of a reduced-wave Green's function and its gradient. Limiting cases of the dynamics are analyzed. For D small with $\varepsilon^2 \ll D \ll 1$, the spike motion is metastable. For $D \gg 1$, the motion now depends on the gradient of a modified Green's function for the Laplacian. The effect of the shape of the domain and of the value of D on the possible equilibrium positions of a one-spike solution is also analyzed. For $D \ll 1$, stable spike-layer locations correspond asymptotically to the centers of the largest radii disks that can be inserted into the domain. Thus, for a dumbbell-shaped domain when $D \ll 1$, there are two stable equilibrium positions near the centers of the lobes of the dumbbell. In contrast, for the range $D \gg 1$ a complex function method is used to derive an explicit formula for the gradient of the modified Green's function. For a specific dumbbell-shaped domain, this formula is used to show that there is only one equilibrium spike-layer location when $D \gg 1$, and it is located in the neck of the dumbbell. Numerical results for other non-convex domains computed from a boundary integral method lead to a similar conclusion regarding the uniqueness of the equilibrium spike location when $D \gg 1$. This leads to the conjecture that, when $D \gg 1$, there is only one equilibrium spike-layer location for any convex or non-convex simply connected domain. Finally, the asymptotic results for the spike dynamics are compared with corresponding full numerical results computed using a moving finite element method.

1 Introduction

In 1952, Turing [24] used a linear stability analysis to show that a pair of reacting and diffusing chemicals modeled by a reaction-diffusion system could evolve from a nearly spatially homogeneous state to a spatially varying state. Subsequently, for many reaction-diffusion systems, it has been shown that small amplitude spatially varying states can evolve to a state where one of the chemicals is concentrated at certain points in the domain (cf. [13], [21], [16]). The resulting patterns are called spike-type patterns. It has been postulated that this chemical concentration phenomena is responsible for a variety of localization processes in nature, such as cell differentiation and biological pattern formation, including the development of some sea shell patterns (cf. [21]).

Since Turing's original work, a great number of reaction-diffusion models have been proposed for pattern formation. One of the most well-known reaction-diffusion systems of this

¹Department of Mathematics, University of British Columbia, Vancouver, Canada V6T 1Z2

²Department of Mathematics, University of British Columbia, Vancouver, Canada V6T 1Z2

type is the Gierer-Meinhardt (GM) model [13], given in dimensionless form by

$$A_t = \varepsilon^2 \Delta A - A + \frac{A^p}{H^q}, \quad x \in \Omega, \quad t > 0, \quad (1.1a)$$

$$\tau H_t = D \Delta H - H + \frac{A^r}{H^s}, \quad x \in \Omega, \quad t > 0, \quad (1.1b)$$

$$\partial_n A = \partial_n H = 0, \quad x \in \partial\Omega. \quad (1.1c)$$

Here Ω is a bounded two-dimensional domain, A and H represent the activator and the inhibitor concentrations, ε^2 and D represent the diffusivity of the activator and inhibitor, τ is the inhibitor time constant, ∂_n denotes the outward normal derivative, and the exponents (p, q, r, s) satisfy

$$p > 1, \quad q > 0, \quad r > 0, \quad s \geq 0, \quad \frac{p-1}{q} < \frac{r}{s+1}. \quad (1.2)$$

In (1.1a) we assume that $\varepsilon \ll 1$ so that the activator diffuses more slowly than does the inhibitor.

The GM system exhibits surprisingly rich dynamics for various parameter ranges. Large amplitude spike solutions have been studied intensively using numerical methods since the 1970's (cf. [13], [21], [16] and references therein), but only relatively recently from an analytical viewpoint.

In this paper we study asymptotically the dynamics of a one-spike solution to the GM system with $\tau = 0$ in the limit $\varepsilon \rightarrow 0$. A one-spike solution has the form shown in Fig. 1. In the analysis, we assume that Ω is a bounded two-dimensional domain. There are many other problems in different areas of science where localized solutions occur and where the dynamics, equilibria, and stability of these solutions is a natural question. Examples of such problems include vortex behavior in superconductivity [20], hot-spots in microwave heating [3], and pulse propagation in chemical patterns [11]. Before describing our specific results for (1.1), we survey some previous results on spike solutions to the GM system in a two-dimensional domain.

When $\tau = 0$ and D is infinite, (1.1) reduces to the well-known shadow system involving a non-local scalar partial differential equation for the activator concentration A . The behavior of spike solutions to this shadow problem is now well understood (see [17], [9], [28]). As $\varepsilon \rightarrow 0$, the equilibrium location of the spike for a one-spike solution is at the center of the largest ball that can be inserted into the domain (cf. [25], [29]). This solution is metastable in the sense that a single spike located in the domain moves exponentially slowly towards the boundary of the domain (cf. [17]). For the equilibrium shadow problem solutions with multiple spikes are possible. The locations of these spikes were found in [2], [14] and [19] to be related to a ball-packing problem. Equilibrium solutions for the shadow problem with two or more spikes are unstable on an $O(1)$ time scale.

In the regime where D is at least logarithmically large as $\varepsilon \rightarrow 0$ (i.e. $D \gg -\ln \varepsilon$ or $D = O(-\ln \varepsilon)$), the stability of an equilibrium n -spike pattern was analyzed rigorously in [30]. This critical level of $O(-\ln \varepsilon)$ is related to the logarithmic behavior of the Green's function in two space dimensions. In [30] it was found that for $\varepsilon \ll 1$ there exists threshold values $D_1 < D_2 < \dots$ such that an n -spike equilibrium solution is stable if and only if $D < D_n$. For the case of a one-spike solution, a differential equation for the dynamics of the center of the spike was derived in [10] and [27] for the case where $D \gg -\ln \varepsilon$.

When D is very small, so that $D = O(\varepsilon^2)$, the motion of two spikes in \mathbb{R}^2 was analyzed in [12]. In this case, both the activator and the inhibitor concentrations are localized near the core of the spikes, with A and H decaying exponentially away from the spike cores. It was found in [12] that the interaction between the spikes is exponentially weak and that the spikes move away from each other with a speed that is exponentially decreasing with the distance between the spike centers. An explicit differential equation for the distance between the spike centers was derived.

There are no results for the dynamics of a spike when D is neither small nor large, i. e. when $D = O(1)$. Recently, when $D = O(1)$, Wei and Winter in [32] and [31] have analyzed the stability of an n -spike equilibrium solution in two dimensions. They found that a stable equilibrium spike pattern will always exist for any finite number of spikes, regardless of the value of D .

A primary goal of this paper is to derive a unified dynamical law that determines the motion of a single spike inside a two-dimensional bounded domain for *any* D with $D \gg \varepsilon^2$. The previous results for large D found in [10] and [27], as well as results for small D , are then obtained as limiting cases. The motion of the spike is found to depend critically on various Green's functions and their gradients.

The equation of motion for a spike for (1.1) when $D = O(1)$ and $\tau = 0$ differs significantly from the case when $D \gg -\ln \varepsilon$, since for $D \gg -\ln \varepsilon$ only the gradient of the regular part of a modified Green's function for the Laplacian is involved (cf. [27]). However, when $D = O(1)$, we find that the differential equation for the spike motion involves both the regular part of a certain reduced-wave Green's function and its gradient. This complication results in part because of the presence of the two different scales, ε and $-\frac{1}{\ln \varepsilon}$, that arise due to the logarithmic point-source behavior of the two-dimensional Green's function. The presence of these two scales makes the asymptotic analysis of the spike motion rather delicate.

The second goal of this paper is to examine how both the shape of the domain and the inhibitor diffusivity constant D determine the possible equilibrium locations for a one-spike solution. We find that for D small, the stable equilibrium spike locations tend to the centers of the disks of largest radii that can fit within the domain. Hence, for D small, there are two stable equilibrium locations for a dumbbell-shaped domain. In contrast, we find that for a certain dumbbell-shaped domain, there is only one possible equilibrium location when D is sufficiently large. To obtain this latter result, we use complex analysis to derive an exact

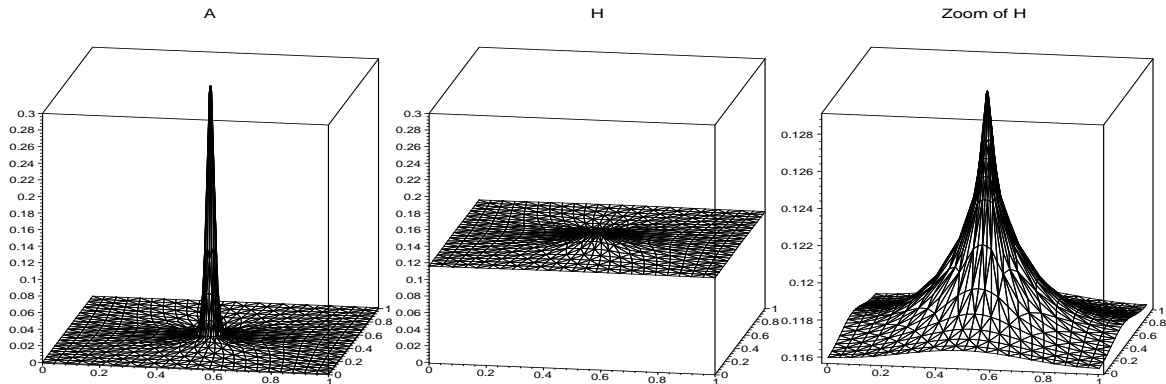


Figure 1: A spike for the Gierer-Meinhardt system (1.1) with $\tau = 0$ in a square domain with $(p, q, r, s) = (2, 1, 2, 0)$ (with A, H rescaled so that both are $O(1)$ as $\varepsilon \rightarrow 0$). Here, $\varepsilon = 0.01$, $D = 5$. Note that H does not change very much compared to A .

expression for the gradient of the modified Green's function for the Laplacian. While this result is obtained for a very specific dumbbell-shaped domain, we conjecture that it is true more generally. More specifically, we conjecture that when D is sufficiently large there is only one possible equilibrium spike location for any simply connected domain. This conjecture is further supported through numerical experiments.

The outline of the paper is as follows. In §2 we introduce an appropriate scaling of (1.1), and we derive the equation of motion for a single spike, which is valid for any D satisfying $D \gg \varepsilon^2$. In §3.1 and §3.2, we then derive limiting results of this evolution for the special cases where $D \ll 1$ and $D \gg -\ln \varepsilon$, respectively. The exact solution for the modified Green's function of the Laplacian on a domain that is an analytic mapping of the unit disk is derived in §4. This result is then applied in §4.1 to a specific dumbbell-shaped domain. In §4.1, a conjecture regarding the uniqueness of the equilibrium spike location for large D is proposed. Numerical evidence supporting this conjecture is given in §4.1 and §5. In §5 we also compare our asymptotic results for the spike motion with corresponding full numerical results. Finally, in §6 we summarize qualitatively the effect of reducing D , and we outline some problems warranting further study.

2 Dynamics Of A One-Spike Solution

In this section we study the dynamics of a one-spike solution to (1.1) when $\tau = 0$. We assume that the spike is centered at some point $x = x_0 \in \Omega$. The goal is to derive a differential equation for the dynamics of $x_0(t)$ for any D with $D \gg \varepsilon^2$.

2.1 A Scaling Analysis

We begin by introducing a rescaled version of (1.1) as was done in [31]. This scaling ensures that the rescaled inhibitor field h is $O(1)$ as $\varepsilon \rightarrow 0$ at $x = x_0 \in \Omega$. To find such a scaling, we let $A(x) = \xi a(x)$ and $H = \xi^{\frac{p-1}{q}} h(x)$, for some constant ξ to be found. With this change of variables, and setting $\tau = 0$ in (1.1b), (1.1) becomes

$$a_t = \varepsilon^2 \Delta a - a + \frac{a^p}{h^q}, \quad x \in \Omega, \quad t > 0, \quad (2.1a)$$

$$0 = D \Delta h - h + \xi^\gamma \frac{a^r}{h^s}, \quad x \in \Omega, \quad t > 0, \quad (2.1b)$$

where γ is defined by

$$\gamma = r + \frac{1}{q}(1-p)(1+s). \quad (2.1c)$$

The parameter ξ will be chosen so that

$$h(x_0) = 1 + o(1), \quad \text{as } \varepsilon \rightarrow 0. \quad (2.2)$$

Since $D \gg \varepsilon^2$, a spike core of extent $O(\varepsilon)$ will be formed near $x = x_0$. In the core, we define a new inner variable $y = \varepsilon^{-1}(x - x_0)$. Outside of the spike core, where $|y| \rightarrow \infty$, the linear terms in (2.1a) dominate, and a decays exponentially as

$$a \sim C \varepsilon^{1/2} |x - x_0|^{-1/2} e^{-|x-x_0|/\varepsilon}, \quad (2.3)$$

for $\varepsilon^{-1}|x - x_0| \rightarrow \infty$. In the core of the spike, we assume that h changes more slowly as $\varepsilon \rightarrow 0$ than does a . This arises from the assumption that $D \gg \varepsilon^2$. In other words, for $\varepsilon \rightarrow 0$, we assume that to a leading order approximation

$$\frac{a(x_0 + \varepsilon y)^r}{h(x_0 + \varepsilon y)^s} \sim \frac{a(x_0 + \varepsilon y)^r}{h(x_0)^s} \sim a(x_0 + \varepsilon y)^r, \quad \frac{a(x_0 + \varepsilon y)^p}{h(x_0 + \varepsilon y)^q} \sim a(x_0 + \varepsilon y)^p. \quad (2.4)$$

Under this assumption, the equilibrium solution to (2.1a) in the limit $\varepsilon \rightarrow 0$ is

$$a(x) \sim w(\varepsilon^{-1}|x - x_0|), \quad (2.5)$$

for some x_0 , where $w(\rho)$ is the unique positive solution of

$$w'' + \frac{1}{\rho} w' - w + w^p = 0, \quad \rho \geq 0, \quad (2.6a)$$

$$w(0) > 0, \quad w'(0) = 0, \quad w \sim c \rho^{-1/2} e^{-\rho}, \quad \text{as } \rho \rightarrow \infty. \quad (2.6b)$$

Here c is a positive constant.

Let $G(x, x_0)$ be the Green's function satisfying

$$\Delta G - \frac{1}{D}G = -\delta(x - x_0), \quad x \in \Omega; \quad \partial_n G = 0, \quad x \in \partial\Omega. \quad (2.7)$$

Let R be the regular part of G defined by

$$R(x, x_0) = G(x, x_0) + \frac{1}{2\pi} \ln |x - x_0|. \quad (2.8)$$

Then, the solution to (2.1b) is

$$h(x_0) = \int_{\Omega} G(x, x_0) \frac{\xi^\gamma a^r(x)}{D h^s(x)} dx. \quad (2.9)$$

Since the integrand in (2.9) is exponentially small except in an $O(\varepsilon)$ region near $x = x_0$, we get from (2.4), (2.5), (2.8) and (2.9), that, as $\varepsilon \rightarrow 0$,

$$h(x_0) \sim \frac{\xi^\gamma \varepsilon^2}{D} \int_{\mathbb{R}^2} \left(-\frac{1}{2\pi} \ln(\varepsilon|y|) + R \right) w^r(|y|) dy = \frac{\xi^\gamma \varepsilon^2 \ln(\frac{1}{\varepsilon})}{2\pi D} \int_{\mathbb{R}^2} w^r(|y|) dy + o(1). \quad (2.10)$$

Thus, to ensure that $h(x_0) = 1 + o(1)$ as $\varepsilon \rightarrow 0$, we must choose ξ as

$$\xi^\gamma = \frac{D\nu}{\varepsilon^2 b}, \quad (2.11)$$

where b and ν are defined as

$$b = \int_0^\infty w^r(\rho) \rho d\rho, \quad \nu = \frac{1}{\ln(\frac{1}{\varepsilon})} \gg \varepsilon, \quad \text{as } \varepsilon \rightarrow 0. \quad (2.12)$$

Substituting (2.11) into (2.1) we obtain the scaled system

$$a_t = \varepsilon^2 \Delta a - a + \frac{a^p}{h^q}, \quad x \in \Omega, \quad t > 0, \quad (2.13a)$$

$$0 = D \Delta h - h + \frac{D\nu a^r}{b\varepsilon^2 h^s}, \quad x \in \Omega, \quad t > 0. \quad (2.13b)$$

2.2 Spike Dynamics For Any D

Next, we derive a differential equation for the motion of the center x_0 of the spike. Our main result is the following:

Proposition 2.1 *Suppose that $D \gg \varepsilon^2$. Then, the trajectory $x = x_0(t)$ of the center of a one-spike solution to (2.13) satisfies the differential equation*

$$\frac{dx_0}{dt} \sim - \left(\frac{4\pi q}{p-1} \right) \frac{\varepsilon^2}{\ln(\frac{1}{\varepsilon}) + 2\pi R_0} \nabla R_0, \quad \text{as } \varepsilon \rightarrow 0, \quad (2.14)$$

where R_0 and its gradient are defined by

$$R_0 \equiv R(x_0, x_0), \quad \nabla R_0 \equiv \nabla_x R(x, x_0)|_{x=x_0}. \quad (2.15)$$

Here R is the regular part of the reduced wave Green's function defined by (2.7) and (2.8).

We now derive this result using the method of matched asymptotic expansions. Assuming that a decays exponentially away from $x = x_0$, we have that a^r/h^s decays exponentially away from x_0 . Thus, from (2.13b), we obtain that the outer solution for h satisfies

$$\Delta h - \frac{h}{D} \sim -2\pi\nu B\delta(x - x_0), \quad B = \frac{1}{2\pi b} \int_{\mathbb{R}^2} \frac{a^r(x_0 + \varepsilon y)}{h^s(x_0 + \varepsilon y)} dy, \quad (2.16)$$

where $B \rightarrow 1$ as $\varepsilon \rightarrow 0$. The solution to (2.16) is

$$h \sim 2\pi B\nu G(x, x_0) = B\nu [-\ln(\varepsilon|y|) + 2\pi R(x_0 + \varepsilon y, x_0)], \quad (2.17)$$

where $y = \varepsilon^{-1}(x - x_0)$ and G satisfies (2.7). The local behavior of the outer solution near the core of the spike is

$$h \sim B + 2\pi\nu B R_0 - \nu B \ln|y| + 2\pi\varepsilon\nu B \nabla R_0 \cdot y + O(\varepsilon^2|y|^2\nu), \quad \text{as } x \rightarrow x_0. \quad (2.18)$$

The difficulty in matching an inner solution to the local behavior of the outer solution given in (2.18) is that there are two scales, ν and ε , to consider. To allow for these two scales, we must expand the inner solution in a generalized asymptotic expansion of the form

$$a = a_0(|y|; \nu) + \varepsilon\nu a_1(y; \nu) + \dots, \quad h = h_0(|y|; \nu) + \varepsilon\nu h_1(y; \nu) + \dots, \quad (2.19)$$

where

$$y = \varepsilon^{-1} [x - x_0(\tau)], \quad \tau = \varepsilon^2\nu t. \quad (2.20)$$

Generalized asymptotic expansions of the form (2.19) have been used in [23] and [26] to treat related singularly perturbed problems involving the two scales ν and ε .

Substituting (2.19) and (2.20) into (2.13), and collecting powers of ε , we obtain

$$\Delta a_0 - a_0 + \frac{a_0^p}{h_0^q} = 0, \quad \Delta h_0 + \frac{\nu a_0^r}{b h_0^s} = 0, \quad |y| \geq 0, \quad (2.21)$$

and

$$\Delta a_1 - a_1 + \frac{pa_0^{p-1}}{h_0^q} a_1 = \frac{qa_0^p}{h_0^{q+1}} h_1 - a_0' \frac{y \cdot x_0'(\tau)}{|y|}, \quad (2.22a)$$

$$\Delta h_1 + \frac{\nu}{b} \left(\frac{ra_0^{r-1}}{h_0^s} a_1 - \frac{sa_0^r}{h_0^{s+1}} h_1 \right) = 0. \quad (2.22b)$$

Here the prime on a_0 indicates differentiation with respect to $|y|$. The matching condition is that $a_i \rightarrow 0$ exponentially as $|y| \rightarrow \infty$ and that h satisfies (2.18) as $|y| \rightarrow \infty$.

We first study the problem (2.21) for the radially symmetric solution a_0 and h_0 . Since the outer inhibitor field is to satisfy $h(x_0) = 1 + o(1)$ as $\varepsilon \rightarrow 0$, we expand the solution to (2.21) as

$$h_0 = 1 + \nu h_{01}(|y|) + O(\nu^2), \quad a_0 = w(|y|) + \nu a_{01}(|y|) + O(\nu^2). \quad (2.23)$$

Here w is defined in (2.6). Substituting (2.23) into (2.21), we obtain for $|y| \geq 0$ that

$$\Delta a_{01} - a_{01} + pw^{p-1} a_{01} = qw^p h_{01}, \quad (2.24a)$$

$$\Delta h_{01} + \frac{1}{b} w^r = 0. \quad (2.24b)$$

The matching process then proceeds as in [23] (see also [26]). Since $\nu \gg \varepsilon$, we treat ν as a constant of order one in the local behavior of the outer solution given in (2.18). We now match the constant term of the inner solution h_0 to the constant term of the local behavior of the outer solution (2.18). This yields $1 = B + \nu 2\pi B R_0$, so that

$$B = \frac{1}{1 + 2\pi R_0 \nu}. \quad (2.25)$$

Substituting this value of B back into (2.18), we then obtain the revised matching condition

$$h \sim 1 - \frac{\nu}{1 + 2\pi \nu R_0} \ln |y| + 2\pi \varepsilon \nu B \nabla R_0 \cdot y + \dots, \quad \text{as } y \rightarrow \infty, \quad (2.26)$$

where B is given in (2.25). Expanding (2.26) in a Taylor series in ν , and comparing with the expansion of h_0 in (2.23), we conclude that h_{01} must satisfy (2.24b) subject to the far-field asymptotic behavior

$$h_{01} = -\ln |y| + o(1), \quad \text{as } |y| \rightarrow \infty. \quad (2.27)$$

Recalling the definition of b in (2.12), it easily follows that there is a unique solution to (2.24b) with asymptotic behavior (2.27). Solving for h_{01} , and then substituting into (2.24a), we can then in principle determine a_{01} . Higher order terms in the logarithmic expansion of a_0 and h_0 can be obtained in the same way.

We now study the problem (2.22) for a_1 and h_1 . From the matching condition (2.26) it follows that we must have $h_1 = 2\pi B \nabla R_0 \cdot y + o(1)$ as $|y| \rightarrow \infty$. Thus, we introduce \tilde{h}_1 by

$$h_1 = 2\pi B \nabla R_0 \cdot y + \tilde{h}_1, \quad (2.28)$$

where $\tilde{h}_1 \rightarrow 0$ as $|y| \rightarrow \infty$. Substituting (2.28) into (2.22), we can write the resulting system in matrix form as

$$\mathbf{L}\phi + \mathcal{M}\phi = \mathbf{f}, \quad \mathcal{M} \equiv \begin{pmatrix} m_{11} & m_{12} \\ m_{21} & m_{22} \end{pmatrix}, \quad \phi \equiv \begin{pmatrix} a_1 \\ \tilde{h}_1 \end{pmatrix}, \quad \mathbf{f} \equiv \begin{pmatrix} f_1 \\ f_2 \end{pmatrix}, \quad (2.29)$$

where \mathbf{L} is the Laplacian operator $\mathbf{L}\phi \equiv \Delta\phi$, and

$$m_{11} = -1 + \frac{pa_0^{p-1}}{h_0^q}, \quad m_{12} = -\frac{qa_0^p}{h_0^{q+1}}, \quad (2.30a)$$

$$m_{21} = \frac{\nu r a_0^{r-1}}{bh_0^s}, \quad m_{22} = -\frac{\nu s a_0^r}{bh_0^{s+1}}, \quad (2.30b)$$

$$f_1 = 2\pi q B \nabla R_0 \cdot y \frac{a_0^p}{h_0^{q+1}} - a_0' \frac{y \cdot x_0'(\tau)}{|y|}, \quad f_2 = 2\pi \nu s B \nabla R_0 \cdot y \frac{a_0^r}{bh_0^{s+1}}. \quad (2.30c)$$

The solution to (2.29) must satisfy $\phi \rightarrow \mathbf{0}$ as $|y| \rightarrow \infty$.

To derive the differential equation for $x_0(t)$ we impose a solvability condition on (2.29). Let ψ be any solution to the homogeneous adjoint problem associated with (2.29). Thus, ψ satisfies,

$$\mathbf{L}\psi + \mathcal{M}^t\psi = \mathbf{0}, \quad (2.31)$$

with $\psi \rightarrow \mathbf{0}$ as $|y| \rightarrow \infty$, where \mathcal{M}^t indicates the transpose of \mathcal{M} . Multiplying (2.29) by ψ^t , we integrate by parts over \mathbb{R}^2 to obtain

$$\int_{\mathbb{R}^2} (\psi^t \mathbf{L}\phi + \psi^t \mathcal{M}\phi) dy = \int_{\mathbb{R}^2} \phi^t (\mathbf{L}\psi + \mathcal{M}^t\psi) dy = \int_{\mathbb{R}^2} \psi^t \mathbf{f} dy. \quad (2.32)$$

Since ψ satisfies the homogeneous adjoint problem, we conclude from (2.31) and (2.32) that (2.29) must satisfy the solvability condition

$$\int_{\mathbb{R}^2} \psi^t \mathbf{f} dy = 0. \quad (2.33)$$

We now obtain a more convenient form for this solvability condition. Setting $\psi = (\psi_1, \psi_2)^t$, and using (2.30a) and (2.30b), we write the adjoint problem (2.31) as

$$\Delta\psi_1 + \left(-1 + \frac{pa_0^{p-1}}{h_0^q}\right)\psi_1 + \frac{\nu r a_0^{r-1}}{bh_0^s}\psi_2 = 0, \quad (2.34a)$$

$$\Delta\psi_2 - \frac{qa_0^p}{h_0^{q+1}}\psi_1 - \frac{\nu s a_0^r}{bh_0^{s+1}}\psi_2 = 0, \quad (2.34b)$$

where $\psi_j \rightarrow 0$ as $|y| \rightarrow \infty$ for $j = 1, 2$. Using (2.30c), the solvability condition (2.33) can be written as

$$x'_0 \cdot \int_{\mathbb{R}^2} \frac{y}{|y|} a'_0 \psi_1 dy = 2\pi B \nabla R_0 \cdot \int_{\mathbb{R}^2} y \left(\frac{q a_0^p}{h_0^{q+1}} \psi_1 + \frac{\nu s a_0^r}{b h_0^{s+1}} \psi_2 \right) dy. \quad (2.35)$$

Equation (2.35) is simplified further by using (2.34b) to replace the right-hand side of (2.35). This yields,

$$x'_0 \cdot \int_{\mathbb{R}^2} \frac{y}{|y|} a'_0 \psi_1 dy = 2\pi B \nabla R_0 \cdot \int_{\mathbb{R}^2} y \Delta \psi_2 dy, \quad (2.36)$$

where B is defined in (2.25). Equation (2.36) is an ordinary differential equation for the motion of the center of the spike.

We note that the derivation of (2.36) has not used any expansion of a_0 or h_0 in powers of the logarithmic gauge function ν . In principle, to determine an explicit form for the ODE (2.36) for $x_0(t)$, which contains all the logarithmic terms, we must solve (2.21) for a_0 and h_0 and then compute non-trivial solutions to the adjoint problem (2.34). This is a difficult task. Instead, we will only calculate the leading order term in an infinite logarithmic expansion of ψ_1 and ψ_2 . This requires only the leading order term in the infinite logarithmic expansion of a_0 and h_0 given in (2.23). Therefore, substituting (2.23) and

$$\psi_1 = \psi_{10} + \nu \psi_{11} + O(\nu^2), \quad \psi_2 = \psi_{20} + \nu \psi_{21} + O(\nu^2), \quad (2.37)$$

into (2.34), we obtain the leading order adjoint problem

$$\Delta \psi_{10} + (-1 + p w^{p-1}) \psi_{10} = 0, \quad (2.38a)$$

$$\Delta \psi_{20} - q w^p \psi_{10} = 0. \quad (2.38b)$$

There are two linearly independent solutions to (2.38a). They are

$$\psi_{10} = \partial_{y_j} w, \quad j = 1, 2. \quad (2.39)$$

Substituting (2.39) into (2.38b), we obtain

$$\Delta \psi_{20} = \frac{q}{p+1} [w^{p+1}(|y|)]' \frac{y_j}{|y|}, \quad j = 1, 2. \quad (2.40)$$

The solution to (2.40) is

$$\psi_{20} = \frac{q}{\rho(p+1)} \left(\int_0^\rho s [w(s)]^{p+1} ds \right) \frac{y_j}{|y|}, \quad (2.41)$$

where $\rho = |y|$. Substituting $a_0 \sim w$, (2.39), and (2.40), into the solvability condition (2.36), we obtain

$$x'_0 \cdot \int_{\mathbb{R}^2} \frac{y}{|y|} w' \partial_{y_j} w dy = \frac{2\pi Bq}{p+1} \nabla R_0 \cdot \int_{\mathbb{R}^2} y [w^{p+1}(|y|)]' \frac{y_j}{|y|} dy, \quad j = 1, 2. \quad (2.42)$$

The integrals in (2.42) are evaluated using

$$\int_{\mathbb{R}^2} \frac{y_i y_j}{|y|^2} [w'(|y|)]^2 dy = \pi \delta_{ij} \int_0^\infty \rho [w'(\rho)]^2 d\rho, \quad (2.43a)$$

$$\int_{\mathbb{R}^2} \frac{y_i y_j}{|y|} [w^{p+1}(|y|)]' dy = \pi \delta_{ij} \int_0^\infty \rho^2 [w^{p+1}(\rho)]' d\rho = -2\pi \delta_{ij} \int_0^\infty \rho [w(\rho)]^{p+1} d\rho, \quad (2.43b)$$

where δ_{ij} is the Kronecker symbol. Substituting (2.43) into (2.42), we obtain

$$x'_0(\tau) = -\frac{4\pi Bq}{p+1} \nabla R_0 \left(\frac{\int_0^\infty [w(\rho)]^{p+1} \rho d\rho}{\int_0^\infty [w'(\rho)]^2 \rho d\rho} \right). \quad (2.44)$$

In Appendix B of [27], equation (2.6) was used to calculate the ratio

$$\frac{\int_0^\infty [w(\rho)]^{p+1} \rho d\rho}{\int_0^\infty [w'(\rho)]^2 \rho d\rho} = \frac{p+1}{p-1}. \quad (2.45)$$

Hence (2.44) reduces to

$$x'_0(\tau) = -\frac{4\pi qB}{p-1} \nabla R_0. \quad (2.46)$$

Substituting (2.25) for B into (2.46), and recalling the definition of ν given in (2.12), we recover the main result (2.14) for $x_0(t)$.

There are two important remarks. Firstly, from (2.46) it follows that the center of the spike moves towards the location of a local minimum of R_0 . This minimum depends only on D and not on ε . In the following sections we will explore how this location depends on D . Secondly, as seen from the analysis above, since we have only used the leading order term in the logarithmic expansion of the homogeneous adjoint eigenfunction, the error in (2.14) is of order $O(\nu)$. This error, however, is still proportional to ∇R_0 . In fact, the two integrals in the solvability condition (2.36) are independent of x_0 and the shape of the domain. Thus, even if we had retained higher order terms in the logarithmic expansion of the adjoint eigenfunction, we would still conclude that the equilibrium locations of the spike are at local minima of ∇R_0 , and the spike would follow the same path in the domain as that described by (2.14). The higher order terms in the logarithmic expansion of a_0 , h_0 and the adjoint eigenfunction, only change the time-scale of the motion. However, at first glance, an error proportional to $O(\nu)$ in the time-scale of the asymptotic dynamics seems rather large. This is not as

significant a concern as it may appear, as from the numerical experiments performed in §5 we show that it is the dependence of B on ν as given in (2.25) that allows for a close agreement between the asymptotic and full numerical results for the spike motion.

3 Limiting Cases Of The Dynamics

In this section we consider two limiting cases of result (2.14) for the motion of a spike. In §3.1 we consider the case where $\varepsilon^2 \ll D \ll 1$ and in §3.2 we consider the case $D \gg 1$.

3.1 Dynamics For Small D

In this section we assume that $\varepsilon^2 \ll D \ll 1$. The inequality $\varepsilon^2 \ll D$ was crucial to the derivation of (2.14) in §2. When $D \ll 1$ we can treat D as a small parameter and obtain limiting results from (2.14).

We begin by introducing \tilde{R} defined by

$$\tilde{R}(x, x_0) = G(x, x_0) - V(x), \quad (3.1)$$

where G satisfies (2.7), and V is the free-space Green's function in \mathbb{R}^2 satisfying

$$\Delta V - \lambda^2 V = -\delta(x - x_0), \quad \lambda \equiv \frac{1}{\sqrt{D}}. \quad (3.2)$$

The solution to (3.2) is

$$V(x) = \frac{1}{2\pi} K_0(\lambda|x - x_0|). \quad (3.3a)$$

The asymptotic behavior of $K_0(r)$ for $r \ll 1$ is

$$K_0(r) \sim -\ln r + \ln 2 - \gamma + O(r^2 \ln r), \quad \text{as } r \rightarrow 0. \quad (3.3b)$$

Here γ is Euler's constant. In terms of \tilde{R} , the regular part R_0 defined in (2.15) is

$$R_0 = \tilde{R}(x_0, x_0) - \frac{1}{2\pi}(\ln \lambda - \ln 2 + \gamma), \quad \nabla R_0 = \nabla \tilde{R}(x, x_0)|_{x=x_0}. \quad (3.4)$$

To obtain some insight into the dynamics when D is small, we first consider the case where $\Omega = [0, 1]^2$ is a unit square. Then, using the method of images, we can solve (2.7) explicitly for G for any value of D . This yields

$$\tilde{R}(x, x_0) = \left(\sum_{n=-\infty}^{\infty} \sum_{m=-\infty}^{\infty} V[v_m(h_n(x))] \right) - V(x), \quad (3.5a)$$

where

$$h_n(x) = \begin{cases} (x_1 - n, x_2) & \text{if } n \text{ is even} \\ (n + 1 - x_1, x_2) & \text{if } n \text{ is odd} \end{cases}, \quad v_m(x) = \begin{cases} (x_1, x_2 - m) & \text{if } m \text{ is even} \\ (x_1, m + 1 - x_2) & \text{if } m \text{ is odd} \end{cases}. \quad (3.5b)$$

For D small, such that $\lambda|x - x_0| \gg 1$, the function V decays exponentially as

$$V(x) \sim \frac{1}{2} \frac{1}{\sqrt{2\pi}} [\lambda|x - x_0|]^{-\frac{1}{2}} e^{-\lambda|x - x_0|}, \quad \text{for } \lambda|x - x_0| \gg 1. \quad (3.6)$$

Now suppose that the spike is located at $x_0 = (\frac{1}{2}, \xi)$ with $O(\frac{1}{\lambda}) \ll \xi < \frac{1}{2} - O(\frac{1}{\lambda})$. Then, for $D \ll 1$, we need only retain the two terms $(n, m) = (0, 0)$ and $(n, m) = (0, -1)$ in the series (3.5a). The other terms are exponentially small at the point x_0 in comparison with these terms. Thus, for $\lambda \rightarrow \infty$, we obtain from (3.5a) that

$$\tilde{R}(x, x_0) \sim \frac{1}{2\pi} K_0[\lambda|\tilde{x} - x_0|], \quad \tilde{x} = (x_1, -x_2), \quad x = (x_1, x_2). \quad (3.7a)$$

Now substituting (3.7a) into (3.4), and using the large argument expansion (3.6), we obtain

$$R_0 \sim \frac{1}{4\sqrt{\pi\lambda\xi}} e^{-2\lambda\xi} + \frac{1}{2\pi} (\ln 2 - \gamma - \ln \lambda), \quad 2\nabla R_0 \sim -\frac{1}{2} \sqrt{\frac{\lambda}{\pi\xi}} e^{-2\lambda\xi} \hat{j}, \quad (3.7b)$$

where \hat{j} is a unit vector in the positive x_2 direction. Substituting (3.7b) into (2.14), we obtain an evolution equation for ξ

$$\frac{d\xi}{dt} \sim \frac{q}{p-1} \left(\frac{\varepsilon^2 \sqrt{\pi\lambda}}{\ln 2 - \gamma - \ln[\varepsilon\lambda]} \right) \frac{e^{-2\lambda\xi}}{\sqrt{\xi}}. \quad (3.8)$$

We now make a few remarks. The ODE (3.8) breaks down when $\varepsilon\lambda = O(1)$. This occurs when $D = O(\varepsilon^2)$. Thus, we require that $\varepsilon \ll 1$ and $\lambda \gg 1$, but $\varepsilon\lambda \ll 1$. In this limit, (3.8) shows that ξ is increasing exponentially slowly without bound as t increases. The ODE, however, was derived under the assumption that $O(\frac{1}{\lambda}) \ll \xi < \frac{1}{2} - O(\frac{1}{\lambda})$. When ξ is near the value $\xi = 1/2$, the ODE must be rederived by retaining an additional image point in the infinite sum in (3.5a) corresponding to $(n, m) = (0, 1)$. The effect of this additional term is to ensure that $\xi \rightarrow 1/2$ as $t \rightarrow \infty$. This implies that the spike tends to the center of the square as $t \rightarrow \infty$.

Consider (3.8) with the initial condition $\xi(0) = \xi_0$. To determine the time T for which $\xi(T) = \xi_1$, where $O(\frac{1}{\lambda}) \ll \xi_0 < \xi_1 < \frac{1}{2} - O(\frac{1}{\lambda})$, we integrate (3.8) to obtain

$$\int_{\xi_0}^{\xi_1} \sqrt{\xi} e^{2\lambda\xi} d\xi = \frac{q}{p-1} \left(\frac{\varepsilon^2 \sqrt{\pi\lambda}}{\ln 2 - \gamma - \ln[\varepsilon\lambda]} \right) T. \quad (3.9)$$

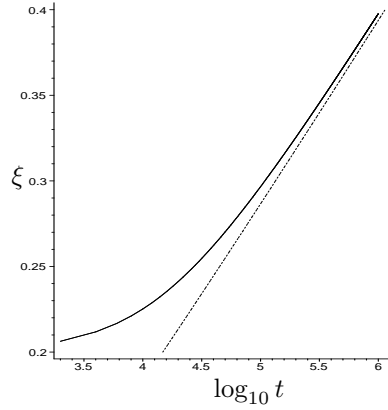


Figure 2: Movement of the center $(0.5, \xi(t))$ of a single spike of (2.13) within a unit box $[0, 1]^2$ versus $\log_{10} t$, with $\varepsilon = D = 0.01$. The solid curve is the numerical solution to (3.8) with $\xi(0) = 0.2$. The broken curve is the approximation (3.10).

Evaluating the integral asymptotically for $\lambda \gg 1$ we get

$$T \sim \frac{p-1}{q} \left(\frac{\ln 2 - \gamma - \ln[\varepsilon\lambda]}{2\varepsilon^2 \sqrt{\pi} \lambda^{3/2}} \right) \sqrt{\xi_1} e^{2\lambda\xi_1}, \quad \lambda \gg 1. \quad (3.10)$$

Thus, when $D \ll 1$, the motion of the spike is *metastable*. The spike moves exponentially slowly with time (see Fig. 2) as it approaches the center of the square. Indeed, this behavior is not specific to a square domain as we will now demonstrate.

More generally, consider any domain Ω with smooth boundary. Let $\tilde{R}(x, x_0)$ be defined as in (3.1). Then, \tilde{R} satisfies

$$\Delta \tilde{R} - \lambda^2 \tilde{R} = 0 \quad x \in \Omega; \quad \partial_n \tilde{R} = -\partial_n V, \quad x \in \partial\Omega, \quad (3.11)$$

where $V(x)$ is given in terms of x_0 by (3.3a). To obtain a representation formula for \tilde{R} , we apply Green's theorem to \tilde{R} and V . This yields,

$$\tilde{R}_0 \equiv \tilde{R}(x_0, x_0) = \int_{\partial\Omega} \left[V(x') \partial_n \tilde{R}(x', x_0) - \tilde{R}(x', x_0) \partial_n V(x') \right] dx'. \quad (3.12)$$

The only term in the integrand of (3.12) that we still need to calculate is $\tilde{R}(x', x_0)$ for $x' \in \partial\Omega$. We now calculate this term for $\lambda \gg 1$ using a boundary layer analysis on (3.11). Since $\lambda \gg 1$, the solution to (3.11) has a boundary layer of width $O(\lambda^{-1})$ near $\partial\Omega$. Thus, it suffices to estimate \tilde{R} inside the boundary layer. Let $\eta = \lambda|x' - x|$ where x' is the point on $\partial\Omega$ closest to x (one can always find such an x' assuming that x is within the boundary

layer and λ is sufficiently large). Let ξ represent the other coordinate orthogonal to η . Then, using this coordinate change in (3.11), we have to leading order that

$$\tilde{R}_{\eta\eta} - \tilde{R} = 0, \quad \eta \geq 0; \quad \lambda \tilde{R}_\eta|_{\eta=0} \sim \partial_n V(x'). \quad (3.13)$$

Since x_0 is assumed to be strictly in the interior of Ω , we can estimate V on $\partial\Omega$ using the far field behavior (3.6). This yields, for $\lambda \gg 1$, that

$$\partial_n V(x') \sim -\lambda V(x') \langle \hat{r}', \hat{n} \rangle, \quad \hat{r}' \equiv \frac{x' - x_0}{|x' - x_0|}, \quad (3.14)$$

where \hat{n} is the unit outward normal to $\partial\Omega$ at x' , and the angle brackets denote the scalar dot product. The solution to (3.13) that is bounded as $\eta \rightarrow +\infty$ is proportional to $e^{-\eta}$. Therefore,

$$\tilde{R} \sim -\lambda^{-1} \partial_n V(x') e^{-\eta}. \quad (3.15)$$

Using (3.14), and evaluating (3.15) on $\partial\Omega$ where $\eta = 0$, we obtain the following key results for $\lambda \gg 1$:

$$\tilde{R}(x', x_0) \sim V(x') \langle \hat{r}', \hat{n} \rangle, \quad x' \in \partial\Omega, \quad (3.16a)$$

$$\partial_n \tilde{R}(x', x_0) \sim \lambda V(x') \langle \hat{r}', \hat{n} \rangle, \quad x' \in \partial\Omega. \quad (3.16b)$$

Next, we substitute (3.16) and (3.14) into (3.12). This yields, for $\lambda \gg 1$, that

$$\tilde{R}_0 \equiv \tilde{R}(x_0, x_0) \sim \lambda \int_{\partial\Omega} \left[V(x') \right]^2 (\langle \hat{r}', \hat{n} \rangle^2 + \langle \hat{r}', \hat{n} \rangle) dx'. \quad (3.17)$$

We now evaluate this integral asymptotically for $\lambda \gg 1$. To do so we use Laplace's formula (see [33]),

$$\int_{\partial\Omega} \frac{1}{r'} F(r') e^{-2\lambda r'} dx' \sim \left(\frac{\pi}{\lambda r_m} \right)^{\frac{1}{2}} e^{-2\lambda r_m} \sum F(r_m) \left(1 - \frac{r_m}{\kappa_m} \right)^{-\frac{1}{2}}. \quad (3.18)$$

Here $r_m = \text{dist}(\partial\Omega, x_0)$, κ_m is the radius of curvature of $\partial\Omega$ at x_m , and the sum is taken over all $x_m \in \partial\Omega$ that are closest to x_0 . The sign convention is such that $\kappa_m > 0$ if Ω is convex at x_m . Comparing (3.17) with (3.18), we get

$$F(r') \equiv \frac{1}{8\pi} (\langle \hat{r}', \hat{n} \rangle^2 + \langle \hat{r}', \hat{n} \rangle). \quad (3.19)$$

At the points $x_m \in \partial\Omega$ closest to x_0 , we have that $r' = r_m$ and $\hat{r}' = \hat{n}$. This yields, $F(r_m) = 1/4\pi$. Therefore, for $\lambda \gg 1$, the estimate (3.18) for (3.17) becomes

$$\tilde{R}_0 \sim \frac{1}{4\sqrt{\lambda\pi r_m}} e^{-2\lambda r_m} \sum \left(1 - \frac{r_m}{\kappa_m} \right)^{-\frac{1}{2}}. \quad (3.20)$$

Finally, to calculate ∇R_0 needed in (2.14), we use (3.4) and the reciprocity relation $\tilde{R}(x, x_0) = \tilde{R}(x_0, x)$ to get

$$\nabla R_0 = \nabla \tilde{R}(x, x_0)|_{x=x_0} = \frac{1}{2} \frac{d}{dx_0} \tilde{R}(x_0, x_0) = \frac{1}{2} \frac{d}{dx_0} \tilde{R}_0. \quad (3.21)$$

Differentiating (3.20), and substituting into (3.21), we obtain

$$2\nabla R_0 \sim \frac{1}{2} \sqrt{\frac{\lambda}{\pi r_m}} e^{-2\lambda r_m} \sum \left(1 - \frac{r_m}{\kappa_m}\right)^{-\frac{1}{2}} \hat{r}_m, \quad (3.22)$$

where $\hat{r}_m \equiv (x_m - x_0)/|x_m - x_0|$. Substituting (3.22) and (3.4) into (2.14), we obtain the following proposition:

Proposition 3.1 *For $\varepsilon^2 \ll D \ll 1$ and $\varepsilon \ll 1$, the trajectory of the center of a one-spike solution to (2.13) satisfies the differential equation*

$$\frac{dx_0}{dt} \sim -\frac{\sqrt{\pi\lambda}q}{p-1} \left(\frac{\varepsilon^2}{\ln 2 - \gamma - \ln[\varepsilon\lambda]} \right) \frac{1}{\sqrt{r_m}} e^{-2\lambda r_m} \sum \left(1 - \frac{r}{\kappa_m}\right)^{-\frac{1}{2}} \hat{r}_m. \quad (3.23)$$

Here $\lambda \equiv D^{-\frac{1}{2}}$, \hat{r}_m is defined following (3.22), and the other symbols are defined in the sentence following (3.18).

Since $r_m = |x_m - x_0|$, we have $\frac{dr_m}{dt} = -\frac{dx_0}{dt} \cdot \hat{r}_m$. From (3.23) this shows that $\frac{dr_m}{dt} > 0$, which implies that the spike moves away from the closest point on the boundary. The formula (3.23) also agrees with (3.8) when Ω is a unit box. Moreover, we have the following result:

Proposition 3.2 *Let $r(x) = \text{dist}(\partial\Omega, x)$. Suppose that x_0 is a local minimum of $f(x_0) \equiv R(x_0, x_0)$ as $\lambda \rightarrow \infty$. Then, for $\lambda \rightarrow \infty$, x_0 is a local maximum of $r(x)$.*

Proof. The proof is by contradiction. Suppose that x_0 is not a local maximum of $r(x)$. Since r is continuous, we can find x_1 with $|x_1 - x_0| > 0$ arbitrary small, with $r(x_1) - r(x_0) > 0$. However, (3.20) yields

$$\frac{\tilde{R}(x_1, x_1)}{\tilde{R}(x_0, x_0)} \sim C e^{-2\lambda[r(x_1) - r(x_0)]}, \quad (3.24)$$

where $C = C(x_0, x_1)$ is independent of λ . Hence, for λ sufficiently large, $\frac{\tilde{R}(x_1, x_1)}{\tilde{R}(x_0, x_0)} < 1$. This implies that $\tilde{R}(x_1, x_1) < \tilde{R}(x_0, x_0)$ for λ large enough. Hence, x_0 is not a local minimizer of \tilde{R} as $\lambda \rightarrow \infty$. Using (3.4) to relate \tilde{R} to R completes the proof. \blacksquare

It follows that for $D \ll 1$ and for convex domains, the center of the spike moves towards a point within the domain located at the center of the largest disk that can be inserted into the domain.

3.2 Dynamics For Large D

The dynamics for the limiting case where $D \gg 1$ is significantly different from the previous analysis where $D \ll 1$.

When D is large, we may expand G defined in (2.7) as

$$G = DG_0 + G_m + \frac{1}{D}G_2 + \cdots. \quad (3.25)$$

Substituting (3.25) into (2.7), and collecting powers of D , we obtain

$$\Delta G_0 = 0, \quad x \in \Omega; \quad \partial_n G_0 = 0, \quad x \in \partial\Omega, \quad (3.26a)$$

$$\Delta G_m = G_0 - \delta(x - x_0), \quad x \in \Omega; \quad \partial_n G_m = 0, \quad x \in \partial\Omega. \quad (3.26b)$$

From (3.26a) we conclude that G_0 is a constant. The solvability condition for (3.26b) then yields

$$G_0 = \frac{1}{\text{vol}\Omega}, \quad (3.27)$$

where $\text{vol}\Omega$ is the area of Ω . The solvability condition for the problem for G_2 also yields that $\int_{\Omega} G_m dx = 0$. Hence, G_m is the modified Green's function for Ω satisfying

$$\Delta G_m = \frac{1}{\text{vol}\Omega} - \delta(x - x_0), \quad x \in \Omega; \quad \partial_n G_m = 0, \quad x \in \partial\Omega; \quad \int_{\Omega} G_m dx = 0. \quad (3.28)$$

Let R_m be the regular part of G_m defined by

$$R_m(x, x_0) = \frac{1}{2\pi} \ln|x - x_0| + G_m(x, x_0). \quad (3.29)$$

Combining (2.8), (3.25), (3.27), and (3.29), we conclude that for $D \gg 1$

$$R(x, x_0) \sim \frac{D}{\text{vol}\Omega} + R_m(x, x_0) + O(1/D). \quad (3.30)$$

Substituting (3.30) into (2.14), we obtain the following proposition:

Proposition 3.3 *If $D \gg 1$ and $\varepsilon \ll 1$, the trajectory of a one-spike solution of (2.13) satisfies*

$$\frac{dx_0}{dt} = -\frac{4\pi q\varepsilon^2}{p-1} \left(\frac{1}{-\ln\varepsilon + 2\pi\frac{D}{\text{vol}\Omega} + 2\pi R_{m0}} \right) \nabla R_{m0}, \quad (3.31a)$$

where R_{m0} and its gradient are defined by

$$R_{m0} \equiv R_m(x_0, x_0), \quad \nabla R_{m0} = \nabla_x R_m(x, x_0)|_{x=x_0}. \quad (3.31b)$$

As a corollary, we obtain the following proposition, which was originally derived in [10] and [27]:

Proposition 3.4 (*Ward et al, [27], Proposition 3.2*) *Let $\varepsilon \ll 1$ and assume that $D \gg -\ln \varepsilon$. Then, the trajectory of a one-spike solution of (2.13) satisfies*

$$\frac{dx_0}{dt} = - \left(\frac{2q \operatorname{vol} \Omega}{p-1} \right) \frac{\varepsilon^2}{D} \nabla R_{m0}, \quad (3.32)$$

where R_{m0} and ∇R_{m0} are defined in (3.31b).

Several general observations can be made by comparing (2.14), (3.23), and (3.32). Firstly, in all three cases, the activator diffusivity ε only controls the timescale of the motion. The precise trajectory traced by x_0 as t increases depends only on D and on the shape of the domain inherited through the terms ∇R_0 and ∇R_{m0} . For the case of small D , where $\varepsilon^2 \ll D \ll 1$, the motion is exponentially slow, or *metastable*, and D controls the dynamics. In contrast, when $D = O(1)$, the speed of the spike is of the order $\frac{\varepsilon^2}{-\ln \varepsilon}$, with a complicated dependence on D through R_0 . Finally for $D \gg -\ln \varepsilon$, the speed is controlled by both ε and D and is of order $\frac{\varepsilon^2}{D}$. In the limit $D \rightarrow \infty$ and $\tau = 0$, the system (1.1) is approximated by the so-called *shadow system* (see [17], [9]). In this case the motion of the spike is again metastable. However, for the shadow system a one-spike interior equilibrium solution is unstable and the spike moves towards the closest point on the boundary of the domain. This behavior is in direct contrast to what we have found for small D , whereby by Propositions 3.1 and 3.2 the spike moves exponentially slowly towards a point that is the furthest away from the boundary. This suggests that as D is increased, the number of possible equilibria for x_0 may decrease. In §4.1 we will show that for a certain dumbbell-shaped domain, there is only one possible stable equilibrium location for D sufficiently large, whereas there are two stable equilibrium locations when D is sufficiently small.

4 Exact Calculation Of The Modified Green's Function

In this section we will use complex analysis to derive an exact formula for ∇R_{m0} defined in (3.31b) for domains of the form

$$\Omega = f(B), \quad (4.1)$$

where B is the unit circle, and f is a rather general class of analytic functions. We will then use this formula to further explore the dynamics of a spike for the GM system on a certain dumbbell-shaped domain. Our main result here is the following:

Theorem 4.1 *Let $f(z)$ be a complex mapping of the unit disk B satisfying the following conditions:*

- (i) f is analytic and is invertible on \overline{B} . Here \overline{B} is B together with its boundary ∂B .
- (ii) f has only simple poles at the points z_1, z_2, \dots, z_k , and f is bounded at infinity.
- (iii) $f = g/h$ where both g and h are analytic on the entire complex plane, with $g(z_i) \neq 0$.
- (iv) $\overline{f(z)} = f(\overline{z})$.

On the image domain $\Omega = f(B)$, let G_m and R_m be the modified Green's function and its regular part, as defined in (3.28) and (3.29), respectively. Let R_{m0} and ∇R_{m0} be the value of R_m and its gradient evaluated at x_0 , as defined in (3.31b). Then, we have

$$\nabla R_{m0} = \frac{\nabla s(z_0)}{f'(z_0)}, \quad (4.2)$$

where $z_0 \in B$ satisfies $x_0 = f(z_0)$, and $\nabla s(z_0)$ is given by

$$\begin{aligned} \nabla s(z_0) = & \frac{1}{2\pi} \left(\frac{z_0}{1 - |z_0|^2} + \frac{f''(\overline{z_0})}{2f'(\overline{z_0})} \right) \\ & \frac{f'(\overline{z_0}) \left(f(z_0) - f\left(\frac{1}{\overline{z_0}}\right) \right) + \sum_j \frac{g(z_j)f'(\frac{1}{z_j})}{z_j^2 h'(z_j)} \left(\frac{1}{z_j - \overline{z_0}} + \frac{z_j}{1 - z_j \overline{z_0}} \right)}{2\pi \sum_j \frac{g(z_j)f'(\frac{1}{z_j})}{z_j^2 h'(z_j)}}. \end{aligned} \quad (4.3)$$

In the equation above, and for the rest of this section, we will treat vectors $v = (v_1, v_2)$ as complex numbers $v_1 + iv_2$. Thus vw is assumed to be complex multiplication. The dot product will be denoted by $\langle v, w \rangle \equiv \frac{1}{2}(v\overline{w} + \overline{v}w)$.

Proof. Given $x, x_0 \in \Omega$, choose z, z_0 such that $x = f(z), x_0 = f(z_0)$. We will use \hat{n} and \hat{N} to denote the normal to ∂B at a point z and the normal to $\partial\Omega$ at $x = f(z)$, respectively. Since f is analytic on \overline{B} we obtain

$$\hat{N} = \frac{\hat{n}f'(z)}{|f'(z)|} = \frac{zf'(z)}{|f'(z)|}, \quad d\sigma(z) = \frac{dz}{iz}, \quad (4.4)$$

where $d\sigma$ is the length element on ∂B .

We now define $S(x)$ by

$$S(x) = G_m(x, x_0) + \frac{1}{2\pi} \ln |x - x_0| - \frac{1}{4 \text{vol} \Omega} |x - x_0|^2. \quad (4.5)$$

Substituting (4.5) into (3.28), we find that S satisfies

$$\begin{cases} \Delta S = 0, & \text{in } \Omega, \\ \langle \nabla S, \hat{N} \rangle = \langle x - x_0, \hat{N} \rangle \left(\frac{1}{2\pi|x-x_0|^2} - \frac{1}{2 \text{vol} \Omega} \right), & \text{on } \partial\Omega, \end{cases} \quad (4.6a)$$

with

$$\int_{\Omega} S dx = \frac{1}{2\pi} \int_{\Omega} \ln |x - x_0| - \frac{1}{4 \text{vol } \Omega} \int_{\Omega} |x - x_0|^2 dx. \quad (4.6b)$$

Combining (4.5) and (3.29), we relate ∇R_m to ∇S as

$$\nabla R_m(x, x_0)|_{x=x_0} = \nabla S(x_0). \quad (4.7)$$

The problem (4.6a) determines S up to an additive constant. This constant is determined by (4.6b). However, the precise value of this additive constant does not influence ∇R_{m0} , since this term depends only on the gradient of S . Hence, without loss of generality, in the derivation below we only calculate S up to an additive constant.

Let $s(z) = S(f(z))$. Since f is analytic and S is harmonic, s satisfies Laplace's equation. Using (4.4), and the fact that f is analytic, we get $\langle \nabla s, \hat{n} \rangle = \langle \nabla S, \hat{N} \rangle |f'(z)|$. Hence, (4.6a) transforms to

$$\begin{cases} \Delta s = 0, & \text{in } B, \\ \langle \nabla s, \hat{n} \rangle = \chi(z, z_0) \equiv \langle x - x_0, z f'(z) \rangle \left(\frac{1}{2\pi |x - x_0|^2} - \frac{1}{2 \text{vol } \Omega} \right), & \text{on } \partial B. \end{cases} \quad (4.8)$$

On the unit ball $\Omega = B$, let $g_m(z, \xi)$ be the solution to the modified Green's function problem (3.28), with singular point at $z = \xi$. It [27] it was shown that

$$g_m(z, \xi) = \frac{1}{2\pi} \left(\frac{|z|^2}{2} - \ln |z - \xi| - \ln \left| z - \frac{\xi}{|\xi|^2} \right| \right) + C(\xi), \quad (4.9)$$

where C is a constant depending on ξ . Notice that if $|z| = 1$ then $|z - \frac{\xi}{|\xi|^2}|^2 = \frac{|z - \xi|^2}{|\xi|^2}$. Hence,

$$\nabla_{\xi} g_m(z, \xi)|_{z \in \partial B} = \frac{1}{\pi} \frac{z - \xi}{|z - \xi|^2} + C_1(\xi), \quad (4.10)$$

where C_1 is another constant.

Next, we use Green's identity to represent the solution to (4.8) as the boundary integral

$$s(\xi) = \int_{\partial B} g_m(z, \xi) \chi(z, z_0) d\sigma(z) + C_2, \quad \chi(z, z_0) \equiv \langle \nabla s, \hat{n} \rangle, \quad (4.11)$$

where C_2 is a constant. Since $s(z) = S(f(z))$, we get from (4.7) that

$$\nabla R_{m0} \equiv \nabla R_m(x, x_0)|_{x=x_0} = \frac{\nabla s(z)}{f'(z)} \Big|_{z=z_0}. \quad (4.12)$$

Differentiating (4.11) with respect to ξ and using (4.10), we evaluate the resulting expression at $\xi = z_0$ to get

$$\nabla s(z_0) = \int_{\partial B} \nabla_{\xi} g_m(z, z_0) \chi(z, z_0) d\sigma = \frac{1}{\pi} \int_{\partial B} \frac{z - z_0}{|z - z_0|^2} \chi(z, z_0) d\sigma + C_1 \int_{\partial B} \chi(z, z_0) d\sigma. \quad (4.13)$$

From (4.8) it follows that $\int_{\partial B} \chi(z, z_0) d\sigma(z) = 0$. Then, using (4.8) for $\chi(z, z_0)$ and (4.4) for $d\sigma(z)$, (4.13) becomes

$$\begin{aligned}
\nabla s(z_0) &= \int_{\partial B} \langle x - x_0, z f'(z) \rangle \left(\frac{1}{2\pi|x - x_0|^2} - \frac{1}{2 \operatorname{vol} \Omega} \right) \frac{1}{\pi} \frac{z - z_0}{|z - z_0|^2} \frac{dz}{iz} \\
&= \frac{1}{2\pi i} \int_{\partial B} \left((x - x_0) \overline{z f'(z)} + \overline{x - x_0} z f'(z) \right) \left(\frac{1}{2\pi|x - x_0|^2} - \frac{1}{2 \operatorname{vol} \Omega} \right) \frac{1}{1 - z\bar{z}_0} dz \\
&= \frac{1}{4\pi^2 i} \int_{\partial B} \left(\frac{z f'(z)}{x - x_0} \right) \frac{1}{1 - z\bar{z}_0} dz + \frac{1}{4\pi^2 i} \int_{\partial B} \frac{z f'(z)}{x - x_0} \frac{1}{1 - z\bar{z}_0} dz \\
&\quad - \frac{1}{4\pi i \operatorname{vol} \Omega} \int_{\partial B} (x - x_0) \overline{z f'(z)} \frac{1}{1 - z\bar{z}_0} dz - \frac{1}{4\pi i \operatorname{vol} \Omega} \int_{\partial B} \overline{x - x_0} z f'(z) \frac{1}{1 - z\bar{z}_0} dz.
\end{aligned} \tag{4.14a}$$

This equation is written concisely as

$$\nabla s(z_0) = J_1 + J_2 + J_3 + J_4, \tag{4.14b}$$

where the J_k are, consecutively, the four integrals in the last equality in (4.14a). We now calculate each of these terms.

We first calculate J_2 . Using the residue theorem, the relations $x = f(z)$ and $x_0 = f(z_0)$, and the invertibility of f , we readily calculate that

$$J_2 \equiv \frac{1}{4\pi^2 i} \int_{\partial B} \frac{z f'(z)}{x - x_0} \frac{1}{1 - z\bar{z}_0} dz = \frac{z_0}{2\pi [1 - |z_0|^2]}. \tag{4.15}$$

To calculate J_1 we use an identity. For any function $H(z)$, it is easy to show that

$$\frac{1}{2\pi i} \int_{\partial B} \overline{H(z)} dz = \frac{1}{2\pi i} \int_{\partial B} \overline{H(z)} \frac{1}{z^2} dz. \tag{4.16}$$

This determines J_1 as

$$J_1 \equiv \frac{1}{4\pi^2 i} \int_{\partial B} \overline{\left(\frac{z f'(z)}{x - x_0} \right)} \frac{1}{1 - z\bar{z}_0} dz = \frac{f''(\bar{z}_0)}{4\pi f'(\bar{z}_0)}. \tag{4.17}$$

To show this, we use $z\bar{z} = 1$ for $z \in \partial B$, and (4.16) and (4.17), to get

$$J_1 = \frac{1}{4\pi^2 i} \int_{\partial B} \overline{\left(\frac{f'(z)}{(x - x_0)(z - z_0)} \right)} \frac{1}{z^2} dz = \frac{1}{4\pi^2 i} \int_{\partial B} \frac{f'(z)}{(x - x_0)(z - z_0)} dz. \tag{4.18}$$

Using $x = f(z)$ and $x_0 = f(z_0)$, we write (4.18) as

$$J_1 = \frac{1}{4\pi^2 i} \int_{\partial B} \frac{\phi(z)}{(z - z_0)^2} dz, \quad \phi(z) \equiv \frac{f'(z)(z - z_0)}{f(z) - f(z_0)}. \tag{4.19}$$

The function $\phi(z)$ is analytic in B and $\phi'(z_0) = f''(z_0)/[2f'(z_0)]$. Thus, using the residue theorem, and property (iv) of Theorem 4.1, we get

$$J_1 = \frac{1}{2\pi} \overline{\phi'(z_0)} = \frac{1}{4\pi} \frac{f''(\bar{z}_0)}{f'(\bar{z}_0)}. \quad (4.20)$$

This completes the derivation of (4.17).

To calculate J_3 and J_4 , we need to evaluate $\text{vol } \Omega$ given by

$$\text{vol } \Omega = \int_{\Omega} dx = \int_{\partial\Omega} \frac{1}{2} \langle x, \hat{N} \rangle d\Sigma. \quad (4.21)$$

Using $d\Sigma = |f'(z)|d\sigma$, $x = f(z)$, $z\bar{z} = 1$ on ∂B , and (4.4) for \hat{N} and $d\sigma$, we get

$$\text{vol } \Omega = \frac{1}{4i} \int_{\partial B} \overline{f(z)} f'(z) dz + \frac{1}{4i} \int_{\partial B} \overline{f'(z)} \frac{f(z)}{z^2} dz. \quad (4.22)$$

To evaluate (4.22), J_3 , and J_4 , we need another identity. Let $F(z)$ be any function analytic inside and on the unit disk, and assume that $\overline{F(z)} = F(\bar{z})$. Then

$$I \equiv \frac{1}{2\pi i} \int_{\partial B} \overline{f(z)} F(z) dz = - \sum_j \frac{g(z_j)}{z_j^2 h'(z_j)} F\left(\frac{1}{z_j}\right). \quad (4.23)$$

To show this result, we use (4.16) to write I as

$$I = \frac{1}{2\pi i} \int_{\partial B} \overline{\bar{z}^2 f(z) \overline{F(z)}} \frac{1}{z^2} dz = \frac{1}{2\pi i} \int_{\partial B} \bar{z}^2 f(z) \overline{F(z)} dz. \quad (4.24)$$

Since $z\bar{z} = 1$ and $\overline{F(z)} = F(\bar{z}) = F(1/z)$ on ∂B , we get

$$I = \bar{J}, \quad \text{where} \quad J \equiv \frac{1}{2\pi i} \int_{\partial B} \frac{f(z) F(1/z)}{z^2} dz. \quad (4.25)$$

Then, since $F(1/z)$ is analytic in $|z| \geq 1$ and $f(z)$ is bounded at infinity by property (ii) of Theorem 4.1, we can evaluate J by integrating the integrand of J over the boundary of the annulus $1 \leq |z| \leq R$ and letting $R \rightarrow \infty$. By properties (ii) and (iii) of Theorem 4.1, $f(z) = g(z)/h(z)$ has simple poles at $z = z_j$ with $|z_j| > 1$. Using the residue theorem over the annulus, and letting $R \rightarrow \infty$, we obtain

$$J = - \sum_j \frac{g(z_j)}{z_j^2 h'(z_j)} F\left(\frac{1}{z_j}\right). \quad (4.26)$$

Substituting (4.26) into (4.25) and using $\overline{f(z)} = f(\bar{z})$, $\overline{F(z)} = F(\bar{z})$, and the fact that z_j is a pole of $f(z)$ if and only if \bar{z}_j is, we obtain the result (4.23) for I .

Next, we use (4.16) to write $\text{vol } \Omega$ in (4.22) as

$$\text{vol } \Omega = \frac{\pi}{2} \left[\frac{1}{2\pi i} \int_{\partial B} \overline{f(z)} f'(z) dz + \frac{1}{2\pi i} \int_{\partial B} \overline{f(z)} f'(z) dz \right]. \quad (4.27)$$

Then, using (4.23), we can calculate the two integrals in (4.27) to get

$$\text{vol } \Omega = -\frac{\pi}{2} \sum_j \left(\frac{g(z_j) f'(\frac{1}{z_j})}{z_j^2 h'(z_j)} + \frac{g(\bar{z}_j) f'(\frac{1}{\bar{z}_j})}{\bar{z}_j^2 h'(\bar{z}_j)} \right) = -\pi \sum_j \frac{g(z_j) f'(\frac{1}{z_j})}{z_j^2 h'(z_j)}. \quad (4.28)$$

The last equality above follows from property (iv) of Theorem 4.1, which implies that z_j is a pole of $f(z)$ if and only if \bar{z}_j is.

Next, we evaluate J_4 of (4.14a). We calculate that

$$J_4 \equiv -\frac{1}{4\pi i \text{vol } \Omega} \int_{\partial B} \overline{f(z) - f(z_0)} z f'(z) \frac{1}{1 - z\bar{z}_0} dz = \frac{1}{2 \text{vol } \Omega} \sum_j \frac{g(z_j) f'(\frac{1}{z_j})}{z_j^2 h'(z_j) (z_j - \bar{z}_0)}. \quad (4.29)$$

To obtain this result, we use the fact that $z f'(z)/(1 - z\bar{z}_0)$ is analytic in B to get

$$J_4 = -\frac{1}{2 \text{vol } \Omega} \left(\frac{1}{2\pi i} \int_{\partial B} \overline{f(z)} \frac{z f'(z)}{1 - z\bar{z}_0} dz \right). \quad (4.30)$$

The result (4.29) then follows by using the identity (4.23) in (4.30).

Lastly, we calculate J_3 of (4.14a). We find,

$$\begin{aligned} J_3 &\equiv -\frac{1}{4\pi i \text{vol } \Omega} \int_{\partial B} [f(z) - f(z_0)] \overline{z f'(z)} \frac{1}{1 - z\bar{z}_0} dz \\ &= \frac{1}{2 \text{vol } \Omega} \sum_j \frac{g(z_j) f'(\frac{1}{z_j})}{h'(z_j) z_j (1 - z_j \bar{z}_0)} + \frac{1}{2 \text{vol } \Omega} f'(\bar{z}_0) \left[f(z_0) - f\left(\frac{1}{\bar{z}_0}\right) \right]. \end{aligned} \quad (4.31)$$

To obtain this result, we use (4.16) to rewrite J_3 as

$$\bar{J}_3 = -\frac{1}{2 \text{vol } \Omega} \left(\frac{1}{2\pi i} \int_{\partial B} \overline{f(z) - f(z_0)} F(z) dz \right), \quad F(z) \equiv \frac{f'(z)}{z - z_0}. \quad (4.32)$$

Now we repeat the steps (4.24)–(4.26) used in the derivation of (4.23), except that here we must include the contribution from the simple pole of $F(z)$ at $z = z_0$, which lies inside B . Analogous to (4.25), we obtain

$$J_3 = -\frac{1}{2 \text{vol } \Omega} \left(\frac{1}{2\pi i} \int_{\partial B} \frac{[f(z) - f(z_0)] f'(1/z)}{z^2 (z^{-1} - \bar{z}_0)} dz \right). \quad (4.33)$$

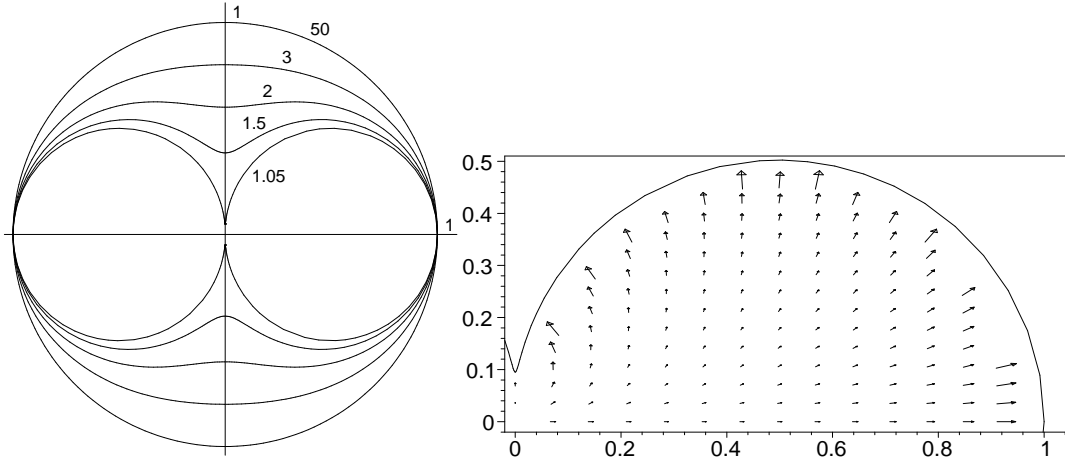


Figure 3: Left: The boundary of $\Omega = f(B)$, with $f(z)$ as given in (4.35), for the values of a as shown. Right: The vector field ∇R_{m0} in the first quadrant of Ω with $a = 1.1$.

Outside the unit disk the integrand has simple poles at $z = z_j$ and at $z = 1/\bar{z}_0$. Integrating over the annulus $1 \leq |z| \leq R$, using the residue theorem, and then letting $R \rightarrow \infty$, we obtain (4.31).

Finally, combining (4.14b) and (4.12), we obtain our result for the gradient of the modified Green's function

$$\nabla R_{m0} \equiv \nabla R_m(x, x_0)|_{x=x_0} = \frac{1}{f'(z_0)} \sum_{k=1}^4 J_k. \quad (4.34)$$

Substituting the results for J_k and $\text{vol } \Omega$ given by (4.15), (4.17), (4.28), (4.29), and (4.31), into (4.34), we obtain our main result (4.2) and (4.3). \blacksquare

4.1 Uniqueness Of The One-Spike Equilibrium Solution For Large D

Consider the following example from [15]:

$$f(z) = \frac{(1 - a^2)z}{z^2 - a^2}. \quad (4.35)$$

Here a is real and $a > 1$. The resulting domain $\Omega = f(B)$ for several values of a is shown in Fig. 3. Notice that $\Omega \rightarrow B$ as $a \rightarrow \infty$. One can also show that as $\varepsilon \equiv a - 1 \rightarrow 0^+$, Ω approaches the union of two circles centered at $(\pm \frac{1}{2}, 0)$, with radius $\frac{1}{2}$, which are connected by a narrow channel of length $2\varepsilon + O(\varepsilon^2)$. From Theorem 4.1, we calculate

$$\nabla s(z_0) = \frac{1}{2\pi} \left(\frac{z_0}{1 - |z_0|^2} - \frac{(\bar{z}_0^2 + 3a^2)\bar{z}_0}{\bar{z}_0^4 - a^4} + \frac{a^2\bar{z}_0}{\bar{z}_0^2 a^2 - 1} + \frac{\bar{z}_0}{\bar{z}_0^2 - a^2} - \frac{(a^4 - 1)^2(|z_0|^2 - 1)(z_0 + a^2\bar{z}_0)(\bar{z}_0^2 + a^2)}{(a^4 + 1)(\bar{z}_0^2 a^2 - 1)(z_0^2 - a^2)(\bar{z}_0^2 - a^2)^2} \right). \quad (4.36)$$

In the limit $a \rightarrow \infty$, $\Omega \rightarrow B$, $x_0 \rightarrow z_0$, and $f'(0) \rightarrow 1$. In this limit, we calculate from (4.2) and (4.36) that

$$\nabla R_{m0} = \frac{1}{2\pi} \left(\frac{2 - |x_0|^2}{1 - |x_0|^2} \right) x_0. \quad (4.37)$$

This is precisely the formula for ∇R_{m0} on the unit disk, which can be derived readily from (4.9) as was done in [27]. This provides an independent verification of a limiting case of Theorem 4.1. We have also verified the formula (4.36) by using the boundary element method to compute ∇R_{m0} for Ω as obtained by the mapping (4.35). The two solutions are graphically indistinguishable.

Next, we calculate from (4.36) that

$$\nabla s(z_0)|_{a \rightarrow 1^+} = \frac{Re(z_0)}{\pi(1 - |z_0|^2)(\bar{z}_0^2 + 1)}. \quad (4.38)$$

In the limit $a \rightarrow 1^+$, Ω becomes the union of two disks of radius $1/2$ centered at $(\pm \frac{1}{2}, 0)$. Thus, the unique root of $\nabla s(z_0)|_{a \rightarrow 1^+} = 0$ in Ω is $z_0 = 0$. This root is easily verified to be a simple root. Hence, it follows from the implicit function theorem that $\nabla s(z_0)$ has a unique root for any $\varepsilon = a - 1 > 0$ small enough. By symmetry, this root must be at the origin. We summarize our result as follows:

Proposition 4.2 *Consider a domain $\Omega = f(B)$ with f given by (4.35) as shown in Fig. 3. Then for $\varepsilon = a - 1 > 0$ small enough, Ω is approximately a union of two disks of radius $\frac{1}{2}$ centered at $(\pm \frac{1}{2}, 0)$, connected by a narrow channel of size $2\varepsilon + O(\varepsilon^2)$. Furthermore, ∇R_{m0} given by (3.31b) has a unique root located at the origin. Thus, in this case, there is a unique equilibrium location for the single-spike solution of (2.13).*

We now show that there are no roots $\nabla s(z_0)$ along the real axis when $a > 1$, except the one at $z_0 = 0$. Thus, there are no equilibrium spike-layer locations in the lobes of the dumbbell for any $a > 1$. In (4.36) we let $z_0 = \bar{z}_0 = \xi$, where $-1 < \xi < 1$. After a tedious but straightforward calculation, we get

$$\nabla s(z_0) = \frac{\xi}{2\pi} \mu(\xi), \quad (4.39a)$$

$$\mu(\xi) \equiv \frac{2a^2(a^2 + 1) - (\xi^2 + a^2)^2}{(a^4 - \xi^4)(1 - \xi^2)} + \frac{1}{a^2\xi^2 - 1} \left[a^2 + \frac{(a^4 - 1)^2(a^2 + 1)(\xi^2 + a^2)(\xi^2 - 1)}{(a^4 + 1)(a^2 - \xi^2)^3} \right]. \quad (4.39b)$$

The function μ is even. Thus, to establish our result, we need only show that $\mu(\xi)$ is of one sign on the interval $0 \leq \xi \leq 1$ for any $a > 1$. A simple calculation shows that the term in the square brackets in (4.39b) vanishes at $\xi = 1/a$. In fact, $\xi = 1/a$ is a removable singularity of μ . It is also easy to show that $\mu(0) > 0$ for any $a > 1$, $\mu \rightarrow +\infty$ as $\xi \rightarrow 1^-$, and $\mu'(\xi) > 0$ on $0 < \xi < 1$. Hence, for any $a > 1$, $\mu(\xi) > 0$ on $0 \leq \xi < 1$. Thus, $\nabla s(z_0)$ has a unique root at $z_0 = 0$. Consequently, there is only one equilibrium spike location, and it is at $z_0 = 0$. This leads us to propose the following conjecture:

Conjecture 4.3 *Let Ω be any simply connected domain, not necessarily convex. Then the gradient ∇R_{m0} of the regular part of the modified Green's function given in (3.31b) has a unique root inside Ω . Thus, there is a unique equilibrium location of a one-spike solution of (2.13).*

In experiments 3 and 4 of §5 we consider another example of a non-convex domain that adds further support to this conjecture.

To illustrate the novelty of our conjecture, we consider a similar problem for the conventional Green's function G_d with Dirichlet boundary conditions satisfying

$$\Delta G_d = -\delta(x - x_0) \quad x \in \Omega, \quad (4.40a)$$

$$G_d = 0, \quad x \in \partial\Omega. \quad (4.40b)$$

The regular part of G_d and its gradient are defined by

$$R_d(x, x_0) = G_d(x, x_0) + \frac{1}{2\pi} \ln |x - x_0|, \quad \nabla R_{d0} = \nabla R_d(x, x_0)|_{x=x_0}. \quad (4.41)$$

It was shown in [15] that

$$f'(z_0)\nabla R_{d0} = -\frac{1}{2\pi} \left(\frac{z_0}{1 - |z_0|^2} + \frac{f''(\bar{z}_0)}{2f'(\bar{z}_0)} \right), \quad (4.42)$$

where $x_0 = f(z_0)$ (compare this result with Theorem 4.1). Unlike computing the modified Green's function R_{m0} with Neumann boundary conditions, no knowledge of the singularities of $f(z)$ outside the unit disk is required to compute $R_{d0} = R_d(x_0, x_0)$.

It was shown by several authors (cf. [15], [5]) that for a *convex* domain Ω , the function R_{d0} is convex. Thus, for convex domains, its gradient has a unique root. However the derivation of this result explicitly uses the convexity of the domain. For non-convex domains generated by the mapping (4.35), it was shown in [15] that ∇R_{d0} can have multiple roots. Thus, the Neumann boundary conditions are essential for Conjecture 4.3.

From Conjecture 4.3 together with (3.32), it follows that for D large enough, there is exactly one possible location for a one-spike equilibrium solution. On the other hand, for a dumbbell-shaped domain such as in Fig. 3, we know from Proposition 3.2, that when D is

small enough, the only possible minima of the regular part R_0 of the reduced wave Green's function are near the centers of the lobes of the two dumbbells. In Appendix A, we show that $R_0 \rightarrow +\infty$ as x_0 approaches the boundary of the domain. Hence, R_0 must indeed have a minimum inside the domain. By symmetry, it follows that for D small enough, the centers of both lobes of the dumbbell correspond to stable equilibrium locations for the spike dynamics. In addition, it also follows by symmetry and by Proposition 3.2 that the origin is an unstable equilibria. Hence, this suggests that a pitchfork bifurcation occurs as D is increased past some critical value D_c . As D approaches D_c from below, the two equilibria in the lobes of the dumbbell should simultaneously merge into the origin. For the non-convex domain of experiment 4 in §5, this qualitative description is verified quantitatively by using a boundary element method to compute R_0 .

5 Numerical Experiments

In this section we perform numerical experiments to verify the asymptotic results of §2 and §3. In experiments 1 and 2 we compare the asymptotic formulas (2.14), (3.31) and (3.32) with corresponding full numerical solutions of (2.13). In experiment 3 we provide some further numerical evidence for Conjecture 4.3.

The asymptotic results require us to compute R_0 , R_{m0} , and their gradients. For experiments 1 and 2 we restrict ourselves to a square domain. For this case R_0 can be computed using the method of images solution (3.5). Equation (3.5) also works well for $D = O(1)$. However, note that the number of terms needed in (3.5) to achieve a specified error bound is directly proportional to D . Therefore the time cost is given by $O(D)$ (the storage cost being constant).

To compute R_0 on a non-square domain (or on a square domain when D is large) as well as to compute R_{m0} on any domain to which Theorem 4.1 does not apply, we have adopted a Boundary Element algorithm as described in §8.5 of [1].

To compare with our asymptotic results we use a finite element method to solve (2.13). A standard numerical finite element method code does not perform well over long time intervals due to the very slow movement of the spike and the very steep gradients near the core of the spike. To overcome this, we have collaborated with Neil Carlson who kindly provided us with his moving-mesh program, `mfe2ds` with adaptive time step (cf. [6], [7]). This has reduced the computer time dramatically, because much fewer mesh nodes or time steps were required. However, the solution obtained from the current version of `mfe2ds`, tends to deviate from the expected solution after a long time period. This is because as the spike moves, it moves the mesh along with it, until eventually the mesh is overstretched (see Fig. 4). In spite of this limitation for long-time computations, full numerical results for (2.13) are computed using `mfe2ds`. Neil Carlson, [8], is currently working on a new version of `mfe2ds` that will incorporate adaptive mesh algorithms to solve this problem.

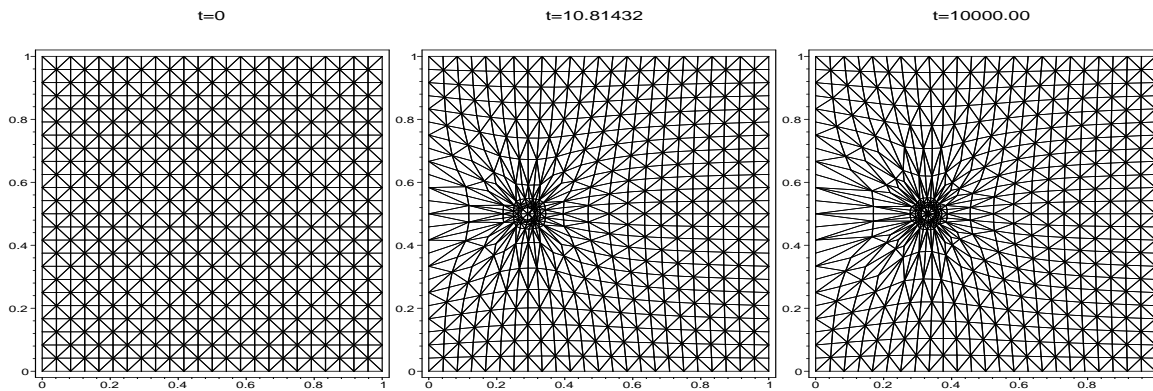


Figure 4: Numerical solution using the moving mesh method. At the beginning, the mesh vertices concentrate at the spike. Then they move along with the spike, eventually overstretching the mesh geometry and resulting in a loss of precision over a long time period. In this example, $\varepsilon = 0.01$, $D = 5$, and the initial conditions at $t = 0$ were $a = \text{sech}(|x - (0.3, 0.5)|)$ and $h = 1$.

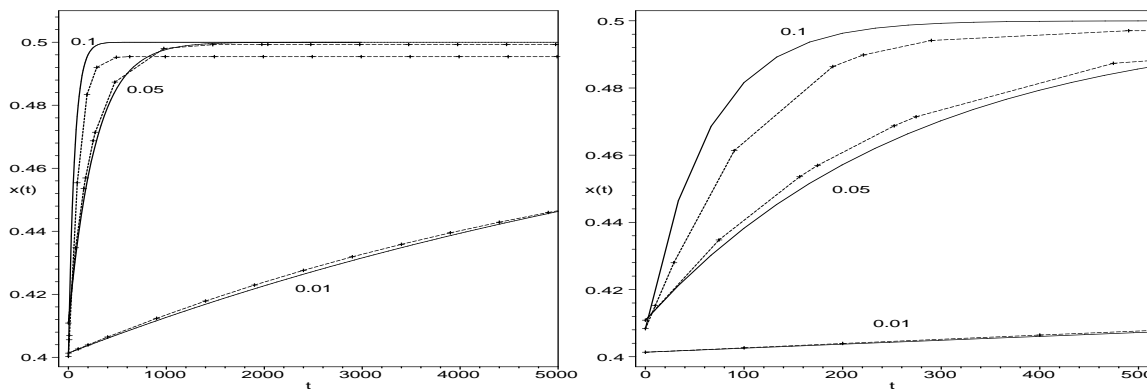


Figure 5: Movement of the center $(x(t), 0.5)$ of a single spike of (2.13) within a unit box $[0, 1]^2$ versus time t . Here $D = 1$ and $\varepsilon = 0.01, 0.05, 0.10$ as shown. The solid lines show the asymptotic approximation (2.14). The broken lines show the full numerical solution computed using `mf2ds`. The figure on the right compares the asymptotic and numerical results on a smaller time interval than the figure on the left.

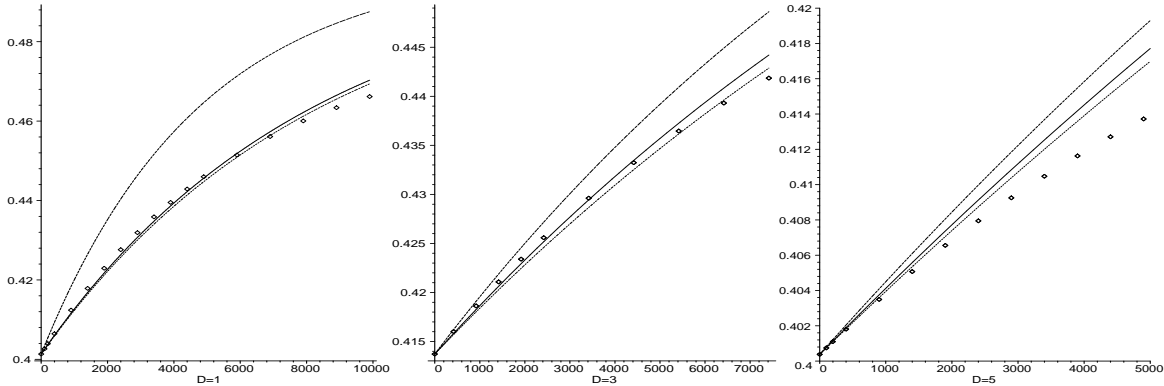


Figure 6: Movement of the center $(x(t), 0.5)$ of a single spike of (2.13) within a unit box $[0, 1]^2$ versus time t , with $\varepsilon = 0.01$ and $D = 1, 3, 5$. The solid curves show the asymptotic approximation (2.14). The bottom and top curves show the approximations (3.31) and (3.32), respectively. The diamonds show the results from the full numerical simulation.

5.1 Experiment 1: Effect Of ε With $D = 1$.

Fig. 5 shows the the peak location $(x(t), 0.5)$ versus time for a unit box $[0, 1]^2$, with $D = 1$ at several values of ε . It shows that the asymptotic approximation (2.14) is very close to the full numerical results when $\varepsilon = 0.01$, and it still gives a reasonable approximation even when $\varepsilon = 0.1$. Presumably, we would have a much closer agreement at $\varepsilon = 0.1$ if we had retained higher order terms in the infinite logarithmic expansion of a_0 , h_0 , and the adjoint eigenfunction ψ , in the derivation of (2.14) from (2.36). From Fig. 5 we note that the full numerical solution for $x(t)$ seems to settle at something less than 0.5. This is a numerical artifact of the current implementation of the moving mesh code. We think that this is caused by the over-stretching of the mesh topology.

5.2 Experiment 2: Effect Of D With $\varepsilon = 0.01$

Fig. 6 shows the peak location $(x(t), 0.5)$ versus time for a unit box $[0, 1]^2$, with $\varepsilon = 0.01$ and $D = 1, 3, 5$. For each value of D , the full numerical solution as well as the asymptotic approximations (2.14), (3.31) and (3.32) are shown.

While we assumed in the derivation of (3.31) that $D \gg 1$, the simulation shows that even for $D = 1$, the approximation (3.31) is rather good. Notice that the approximation (3.32), which does not involve any terms involving $-\ln \varepsilon$ and the modified Green's function in the denominator, provides a significantly worse approximation to the spike dynamics than either (3.31) or (2.14). This point was mentioned at the end of §2.

As before, the numerical solution given by `mfe2ds` seems to deviate from the expected

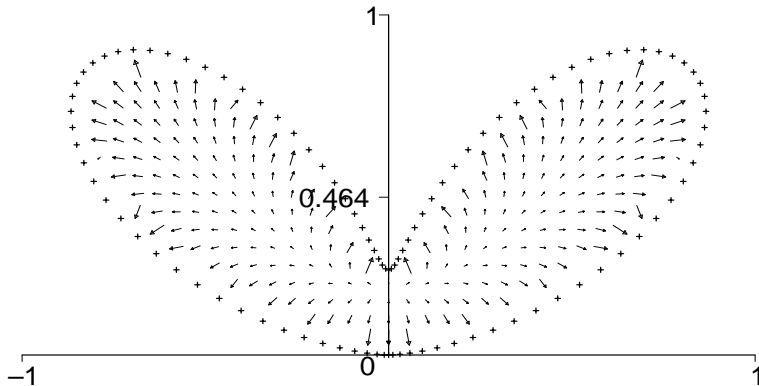


Figure 7: Plot of ∇R_{m0} for a non-convex domain whose boundary is given by $(x, y) = (\sin^2 2t + \frac{1}{4} \sin t)(\cos(t), \sin(t)), t \in [0, \pi]$. Its center of mass is at about $(0, 0.464)$, which lies outside the domain. The resulting vector field has only one equilibrium, at approximately $(0, 0.2)$. The discretization of the boundary that was used for the boundary element method is also shown.

solution after a long time due to excessive mesh stretching. This effect is especially pronounced for larger D . We are currently working with Neil Carlson to address this problem by combining moving mesh with mesh refinement algorithms.

5.3 Experiment 3: Uniqueness Of Equilibria For Large D

We have used a boundary element method to numerically compute ∇R_{m0} for the non-convex domain Ω shown in Fig. 7. There is only one equilibrium solution in Ω and it lies along the imaginary axis as indicated in the figure caption. This provides more evidence for Conjecture 4.3.

5.4 Experiment 4: A Pitchfork Bifurcation.

We consider the non-convex with boundary given by $(x, y) = [2 + \cos(2t)](\cos t, \sin t)$ for $0 \leq t \leq 2\pi$. A plot of the domain is shown in Fig. 8. In this example we use the boundary element method to compute $\partial_x R_0$ along the x axis for different values of λ . Here $R_0 = R(x, x)$ is the regular part of the reduced wave Green's function defined in (2.8). For this domain, there is always a root of $\partial_x R_0$ at the origin. Our goal is to determine if there are any other roots along the real axis. By symmetry we only consider the non-negative x -axis. The results of the computations are shown in Fig. 9. Notice that the scale of the vertical axis in the rightmost plot of Fig. 9 is considerably more compressed than in the leftmost plot. This allows us to see the behavior of $\partial_x R_0$ near the origin. From this figure we notice that a new root of $\partial_x R_0$ emerges from the origin somewhere near $\lambda \approx 1.15$. This gives a critical value

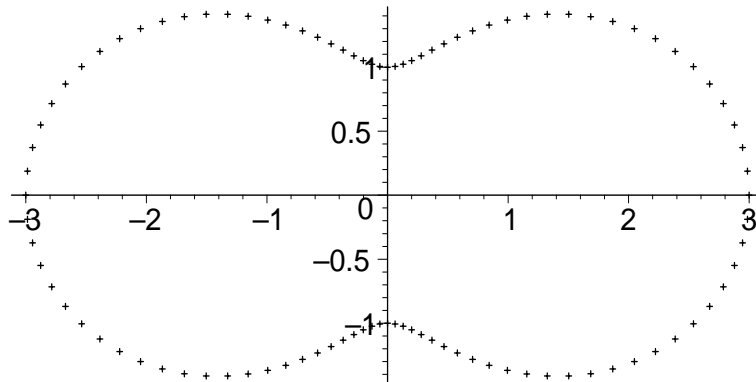


Figure 8: Plot of the non-convex domain of experiment 4 whose boundary is given by $(x, y) = [2 + \cos(2t)](\cos t, \sin t)$ for $0 \leq t \leq 2\pi$.

$D_c \approx 0.756$. For $D > D_c$ the origin is a local minima of R_0 , whereas for $D < D_c$ the origin becomes a local maximum of R_0 . Thus, as D decreases below D_c , the equilibrium spike layer location at the origin loses its stability to two new equilibria, located symmetrically at the points $(x_c(D), 0)$ and $(-x_c(D), 0)$, where $x_c(D) > 0$ and $x_c(D) \rightarrow 0^+$ as $D \rightarrow D_c^-$. This is a classic example of a pitchfork bifurcation.

6 Conclusions

We have analyzed the dynamics and equilibria of an interior spike solution to the GM model in a two-dimensional domain. Qualitatively, there are different dynamical behaviors for different asymptotic ranges of the inhibitor diffusivity D . When $D = \infty$, equilibrium spike locations are at critical points of the distance function, and the resulting equilibrium solutions are metastable (cf. [17], [9]). However, such solutions are ultimately unstable since an interior spike that is slightly offset from its equilibrium position will drift exponentially slowly towards the closest point on the boundary. For the range $\varepsilon^2 \ll D \ll 1$, equilibrium locations for the spike are again at critical points of the distance function. Although the spike motion is again metastable (see proposition 3.1), a spike that is slightly offset from a local maxima of the distance function will drift slowly back towards this point. On the ranges $D = O(1)$, and $D \gg 1$ with D independent of ε , the distance function does not play a prominent role in either the dynamics or equilibria of a spike solution. For $D \gg 1$, the regular part of the modified Green's function for the Laplacian determines the spike dynamics and equilibria. Alternatively, for $D = O(1)$ the regular part of the reduced wave Green's function is central to the analysis. We have derived formal asymptotic results for the motion of a spike when $D = O(1)$ (see proposition 2.1) and when $D \gg 1$ (see propositions 3.2 and

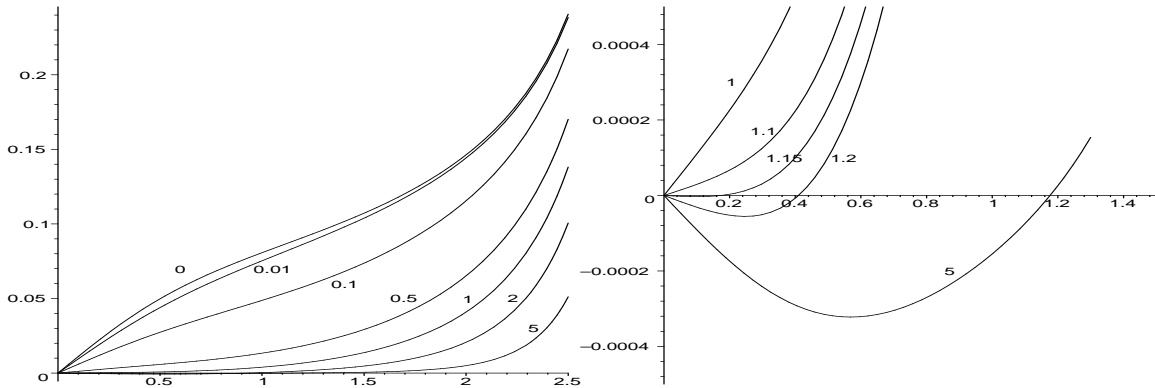


Figure 9: Plot of $\partial_x R_0$ when x is along the positive real axis for the domain of experiment 4. The values of $\lambda = D^{-1/2}$ are shown in the plots. The vertical scale in the rightmost figure is a compression of the scale in the leftmost figure.

3.3). An added complication in the analysis is the presence of $-\log \varepsilon$ terms that arise from the two-dimensional Green's function. These terms, which are important for obtaining close quantitative agreement with full numerical results for spike dynamics, were incorporated into the asymptotic analysis. It is an open problem to give a rigorous proof of propositions 2.1, 3.1, 3.2, and 3.3.

To determine the spike dynamics and equilibrium locations for the asymptotic range $D \gg 1$, we derived rigorously an explicit formula for the gradient of the regular part of the modified Green's function for a class of domains that can be mapped to the unit disk. By using this formula, and by applying it to certain dumbbell-shaped domains, we conjecture (see conjecture 4.3) that the gradient of the regular part of the modified Green's function will vanish exactly once in any simply connected domain. The implication of this conjecture is that when $D \gg 1$ there is only one equilibrium position for a spike solution to the GM model in any simply connected domain. For a particular dumbbell-shaped domain we showed that when $D = O(1)$ the gradient of the regular part of the reduced wave Green's function has three zeroes for D less than some critical value, and that these zeroes experience a pitchfork bifurcation as D is increased past this value. Therefore, it is of considerable interest to examine conjecture 4.3, and to determine, as a function of increasing D , the number of zeroes of the gradient of the regular part of the reduced wave Green's function defined in (2.8) in an arbitrary simply connected domain.

In contrast, many general properties have been established for the regular part of the Green's function for the Laplacian under homogeneous Dirichlet boundary conditions. A survey of results is given in [1]. This latter Green's function plays a prominent role in other problems, including concentration phenomena for Bratu's equation (cf. [22]) and the motion

of vortices for the Ginzburg-Landau equation (cf. [18]). In another context, the regular part of the Green's function for the Helmholtz equation under Dirichlet boundary conditions is shown in [4] to be critical to the analysis of the disappearance of solutions to a nonlinear elliptic problem with critical nonlinearity in a cube. Our analysis of spike motion for the GM model has clearly suggested the need for further work to establish general properties of the regular part of the modified Green's function and the reduced wave Green's function.

Acknowledgements

We would like to thank Neil Carlson for generously providing us his finite element code `mfe2ds` and for his invaluable help in configuring the code for carrying out the computations. We would also like to thank David Iron for helpful discussions about the material in §4. M. J. W. is grateful for the support of NSERC under grant 81541.

A Appendix: The Behavior Of R_0 On The Boundary

Theorem A.1 *Suppose $\partial\Omega$ is C^2 smooth. Let $x' \in \partial\Omega$ and let $x_0(d) = x' - d\hat{n}$ be the point a distance d away from x' and $\partial\Omega$. Then there exist positive constants C_1, C_2, ϵ such that*

$$R(x_0, x_0) \geq C_1 \ln \frac{1}{d} + C_2, \quad (\text{A.1})$$

for all $d \leq \epsilon$ sufficiently small, where R is given by (2.15).

Proof.

When Ω is convex, this theorem was proven in the Appendix of [31]. However, the convexity assumption was critical in their proof. Our proof below does not require this assumption. The proof in [31] utilized a boundary integral representation of R . We use the comparison principle instead.

It suffices to prove this result for R replaced by \tilde{R} . From (2.7) and (3.1), \tilde{R} satisfies

$$\Delta \tilde{R}(x, x_0) - \lambda^2 \tilde{R}(x, x_0) = 0, \quad x \in \Omega; \quad \partial_n \tilde{R}(x, x_0) = -\partial_n V(|x - x_0|), \quad x \in \partial\Omega,$$

where $\lambda \equiv 1/\sqrt{D}$, and

$$V(r) = \frac{1}{2\pi} K_0(\lambda r).$$

By rotating and translating, we may assume that $x_0 = (d, 0)$ and $x' = 0$. We parameterize $\partial\Omega$ by its arclength $x(s)$ with $x(0) = x'$. We let $x_0^r = (-d, 0)$ be the reflection of x_0 in x' and define κ be the curvature of $\partial\Omega$ at x' .

Step 1. Show that

$$\partial_n V(|x - x_0^r|) - C \leq -\partial_n V(|x - x_0|), \quad (\text{A.2})$$

for some constant C , for all $s, d < \varepsilon$, and ε small enough.

If $\kappa > 0$, then it follows geometrically that for ε small enough, $|x - x_0^r| \geq |x - x_0|$ and $-\frac{\langle x - x_0^r, \hat{n} \rangle}{|x - x_0^r|} \leq \frac{\langle x - x_0, \hat{n} \rangle}{|x - x_0|}$. Hence (A.2) follows with $C = 0$ from the monotonicity of V .

The case $\kappa < 0$ is more involved. We have,

$$x(s) = \left(\frac{\kappa}{2}s^2 + o(s^3), s + o(s^3)\right), \quad \hat{n} = (-1 + o(s^2), \kappa s + o(s^2)),$$

where κ is the curvature at x' . Here and below, $o(s^p, d^q)$ is some function such that $o(s^p, d^q) \leq C(|s|^p + |d|^q)$ for some constant C and for all $|s|, |d| \leq \varepsilon$. For $x = x(s)$, we have

$$\langle x - x_0(d), \hat{n} \rangle = \frac{\kappa}{2}s^2 - d + o(s^2)d + o(s^3),$$

and

$$|x - x_0|^2 = d^2 + s^2(1 - \kappa d) + o(s^3).$$

Next, we calculate that

$$\begin{aligned} -\partial_n V(|x - x_0|) &= \frac{1}{2\pi} \frac{\langle x - x_0, \hat{n} \rangle}{|x - x|^2} + o(|x - x_0|) \quad \text{by (3.3b)}, \\ &= \frac{1}{2\pi} \frac{\frac{\kappa}{2}s^2 - d + o(s^2)d + o(s^3)}{d^2 + s^2(1 - \kappa d) + o(s^3)} + o(s, d), \\ &= \frac{1}{2\pi} \frac{\frac{\kappa}{2}s^2 - d + o(s^2)d + o(s^3)}{d^2 + s^2(1 - \kappa d)} \left(1 - \frac{o(s^3)}{d^2 + s^2(1 - \kappa d)} + \dots\right) + o(s, d), \\ &= \frac{1}{2\pi} \left(\frac{\frac{\kappa}{2}s^2 - d}{d^2 + s^2(1 - \kappa d)} + o(s)\right) (1 + o(s)) + o(s, d), \\ &= \frac{1}{2\pi} \frac{\frac{\kappa}{2}s^2 - d}{d^2 + s^2(1 - \kappa d)} + o(s) \frac{d}{d^2 + s^2(1 - \kappa d)} + o(s, d), \\ &= \frac{1}{2\pi} \frac{\frac{\kappa}{2}s^2 - d}{d^2 + s^2} (1 + o(d)) + o(s) \frac{d}{d^2 + s^2} + o(s, d), \\ &= \frac{1}{2\pi} \frac{\frac{\kappa}{2}s^2 - d}{d^2 + s^2} + \frac{o(sd)}{d^2 + s^2} + o(s, d), \\ &= \frac{1}{2\pi} \frac{\frac{\kappa}{2}s^2 - d}{d^2 + s^2} + o(1) + o(s, d). \end{aligned}$$

In a similar way, we get

$$\partial_n V(|x - x_0^r|) = \frac{1}{2\pi} \frac{-\frac{\kappa}{2}s^2 - d}{d^2 + s^2} + o(1) + o(s, d).$$

Therefore,

$$\begin{aligned} -\partial_n V(|x - x_0|) &\geq \frac{1}{2\pi} \frac{\frac{\kappa}{2}s^2 - d}{d^2 + s^2} + C_1, \\ \partial_n V(|x - x_0^r|) &\leq \frac{1}{2\pi} \frac{-\frac{\kappa}{2}s^2 - d}{d^2 + s^2} + C_2, \end{aligned}$$

for some constants C_1, C_2 independent of d, s . Notice that

$$\frac{-\frac{\kappa}{2}s^2 - d}{d^2 + s^2} + \kappa \leq \frac{\frac{\kappa}{2}s^2 - d}{d^2 + s^2} + |\kappa|.$$

Hence,

$$\partial_n V(|x - x_0^r|) + \frac{\kappa - |\kappa|}{2\pi} + C_1 - C_2 \leq -\partial_n V(|x - x_0|),$$

which completes the proof of Step 1.

Step 2. By the compactness of the set $(\partial\Omega \setminus \{x(s), |s| < \epsilon\}) \times \{x_0(d), 0 \leq d \leq \epsilon\}$, the continuity of $V(|x - x_0|)$ on this set, and (A.2), it follows that (A.2) holds for all $x \in \partial\Omega$ and all $d < \epsilon$ if the constant C is large enough.

Step 3. Let $u(x)$ be the solution of

$$\Delta u - \lambda^2 u = 0, \quad x \in \Omega; \quad \partial_n u = -C, \quad x \in \partial\Omega,$$

where C is as in step 2. Then $v = V(|x - x_0^r|) + u$ also satisfies $\Delta v - \lambda^2 v = 0$ and $\partial_n v(x) < \partial_n R(x, x_0)$ for $x \in \partial\Omega$ and any d, ϵ . By the maximum principle, it follows that $v(x) < R(x, x_0)$ for $x \in \Omega$. Recalling (3.3b) completes the proof. \blacksquare

References

- [1] C. Bandle, M. Flucher, *Harmonic Radius and Concentration of Energy; Hyperbolic Radius and Liouville's Equations $\Delta U = e^U$ and $\Delta U = U^{(n+2)/(n-2)}$* , SIAM Rev., **38**, No. 2, (1996), pp. 191–238.
- [2] P. Bates, N. Fusco, *Equilibria with Many Nuclei for the Cahn-Hilliard Equation*, J. Diff. Eq., **160**, No. 2, (2000), pp. 283–356.
- [3] A. Bose, G. Kriegsmann, *Large Amplitude Solutions of Spatially Non-Homogeneous Non-Local Reaction-Diffusion Equations*, Methods and Appl. of Analysis, **7**, No. 2, (2000), pp. 295–312.
- [4] C. J. Budd, A. B. Humphries, A. J. Wathen, *The Finite Element Approximation of Semilinear Elliptic Partial Differential Equations with Critical Exponents in the Cube*, SIAM J. Sci. Comput., **20**, No. 5, (1999), pp. 1875–1904.

- [5] L. A. Caffarelli, A. Friedman, *Convexity of Solutions of Semilinear Elliptic Equations*, Duke Math. J., **52**, No. 2, (1985), pp. 431–456.
- [6] N. N. Carlson, K. Miller, *Design and Application of a Gradient-Weighted Moving Finite Element Code I: in Two Dimensions*, SIAM J. Sc. Comput., **19**, No. 3, (1998), pp. 728–765.
- [7] N. N. Carlson, K. Miller, *Design and Application of a Gradient-Weighted Moving Finite Element Code II: in Two Dimensions*, SIAM J. Sc. Comput., **19**, No. 3, (1998), pp. 766–798.
- [8] N. N. Carlson, private communication.
- [9] X. Chen, M. Kowalczyk, *Slow Dynamics of Interior Spikes in the Shadow Gierer-Meinhardt System*, Adv. in Diff. Equat., **6**, No. 7, (2001), pp. 847–872.
- [10] X. Chen, M. Kowalczyk, *Dynamics of an Interior Spike in the Gierer-Meinhardt System*, SIAM. J. Math. Anal., **33**, No. 1, (2001), pp. 172–193.
- [11] A. Doelman, T. J. Kaper, P. Zegeling, *Pattern Formation in the One-Dimensional Gray-Scott Model*, Nonlinearity, **10**, No. 2, (1997), pp. 523–563.
- [12] S. I. Ei, J. Wei, *Dynamics of Metastable Localized Patterns and its Application to the Interaction of Spike Solutions for the Gierer-Meinhardt System in Two Spatial Dimensions*, Japan J. Ind. Appl. Math., **19**, No. 2, (2002), pp. 181–226.
- [13] A. Gierer, H. Meinhardt, *A Theory of Biological Pattern Formation*, Kybernetik, **12**, (1972), pp. 30–39.
- [14] C. Gui, J. Wei, *Multiple Interior Peak Solutions for Some Singularly Perturbed Neumann Problems*, J. Diff. Eq., **158**, No. 1, (1999), pp. 1–27.
- [15] B. Gustafsson, *On the Convexity of a Solution of Liouville’s Equation*, Duke Math. J., **60**, No. 2, (1990), pp. 303–311.
- [16] L. Harrison, D. Holloway, *Order and Localization in Reaction-Diffusion Pattern*, Physica A, **222**, (1995), pp. 210–233.
- [17] D. Iron, M. J. Ward, *A Metastable Spike Solution for a Non-Local Reaction-Diffusion Model*, SIAM J. Appl. Math., **60**, No. 3, (2000), pp. 778–802.
- [18] S. Jimbo, Y. Morita, *Vortex Dynamics for the Ginzburg Landau Equation with Neumann Condition*, Methods Appl. Anal., **8** No. 3, (2001), pp. 451–477.

- [19] M. Kowalczyk, *Multiple Spike Layers in the Shadow Gierer-Meinhardt System: Existence of Equilibria and Approximate Invariant Manifold*, Duke Math. J., **98**, No. 1, (1999), pp. 59–111.
- [20] F. H. Lin, Q. Du, *Ginzburg-Landau Vortices: Dynamics, Pinning and Hysteresis*, SIAM J. Math. Anal., **28**, No. 6, (1997), pp. 1265–1293.
- [21] H. Meinhardt, *Models of Biological Pattern Formation*, Academic Press, London, (1982).
- [22] K. Nagasaki, T. Suzuki, *Asymptotic Analysis for Two-Dimensional Elliptic Eigenvalue Problems with Exponentially Dominated Nonlinearities*, Asymptotic Anal., **4**, (1990), pp. 173–188.
- [23] M. Titcombe, M. J. Ward, *Summing Logarithmic Expansions for Elliptic Equations in Multiply-Connected Domains with Small Holes*, **7**, No. 3, (1999), pp. 313–343.
- [24] A. Turing, *The Chemical Basis of Morphogenesis*, Phil. Trans. Roy. Soc. B, **237**, (1952), pp. 37–72.
- [25] M. J. Ward, *An Asymptotic Analysis of Localized Solutions for Some Reaction-Diffusion Models in Multi-Dimensional Domains*, Stud. Appl. Math., **97**, No. 2, (1996), pp. 103–126.
- [26] M. J. Ward, W. D. Henshaw, J. B. Keller, *Summing Logarithmic Expansions for Singularly Perturbed Eigenvalue Problems*, SIAM J. Appl. Math., **53**, No. 3, (1993), pp. 799–828.
- [27] M. J. Ward, D. McInerney, P. Houston, D. Gavaghan, P. Maini, *The Dynamics and Pinning of a Spike for a Reaction-Diffusion System*, SIAM J. Appl. Math., **62**, No. 4, (2002), pp. 1297–1328.
- [28] J. Wei, *On Single Interior Spike Solutions for the Gierer-Meinhardt System: Uniqueness and Stability Estimates*, Europ. J. Appl. Math., **10**, No. 4, (1999), pp. 353–378.
- [29] J. Wei, *On the Interior Spike Layer Solutions to a Singularly Perturbed Neumann Problem*, Tohoku Math. J., **50**, No. 2, (1998), pp. 159–178.
- [30] J. Wei, M. Winter, *Spikes for the Two-Dimensional Gierer-Meinhardt System: the Weak Coupling Case*, J. Nonlinear Sci., **11**, No. 6, (2001), pp. 415–458.
- [31] J. Wei, M. Winter, *Spikes for the Two-Dimensional Gierer-Meinhardt System: the Strong Coupling Case*, J. Diff. Eq., **178**, No. 2, (2002), pp. 475–518.
- [32] J. Wei, M. Winter, *On the Two-Dimensional Gierer-Meinhardt System with Strong Coupling*, SIAM J. Math. Anal., **30**, No. 6, (1999), pp. 1241–1263.

- [33] R. Wong, *Asymptotic Approximations of Integrals*, Academic Press, San Diego, CA, (1989).